*Journal of the*

# OPTICAL SOCIETY *of* AMERICA

VOLUME 23
No. 8

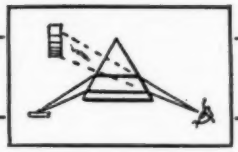

AUGUST
1933

## CONTENTS

**Studies in Refractive Index. III.** A. M. TAYLOR AND DOROTHY A. DURFEE 263

**Infrared Radiations from Small Particles** . . . . . .A. H. PFUND 270

**On the Astigmatism of the Concave Grating** . . . . . .G. H. DIEKE 274

**Method of Projecting Star Images Having Coma and Astigmatism** . . . . .
. . . . . .R. KINGSLAKE AND A. B. SIMMONS 282

**New Optical Experiment and the Use of a Single Lens for High Magnification; Observation of Entoptic and Diffraction Phenomena** . . . . . .
. . . . . .J. GIBSON WINANS 289

**Optical Tests of the 69-Inch Perkins Observatory Reflector** . . . . . .
. . . . . HARLAN T. STETSON 293

*Published monthly*
at Prince and Lemon Sts., Lancaster, Pa.
*by the*
AMERICAN INSTITUTE OF PHYSICS
Incorporated
11 East 38th Street, New York, N. Y.
FOR AND UNDER THE EDITORIAL SUPERVISION OF
THE OPTICAL SOCIETY OF AMERICA

# THE OPTICAL SOCIETY OF AMERICA

## OFFICERS OF THE SOCIETY

E. C. CRITTENDEN, *President*
Bureau of Standards
Washington, D. C.

W. B. RAYTON, *Vice-President*
Bausch & Lomb Optical Company
Rochester, New York

L. B. TUCKERMAN, *Secretary*
Bureau of Standards
Washington, D. C.

HENRY F. KURTZ, *Treasurer*
Bausch & Lomb Optical Company
Rochester, New York

The Council consists of the above officers; the Editor of the Journal; the past President; and four elected members:

L. A. JONES, *Past President*
Eastman Kodak Company
Rochester, New York

F. K. RICHTMYER, *Editor*
Cornell University
Ithaca, New York

*Elected Members*

G. S. FULCHER
Administration Building
World's Fair
Chicago, Illinois

A. C. HARDY
Massachusetts Institute of Technology
Cambridge, Massachusetts

T. R. WILKINS
University of Rochester
Rochester, New York

A. G. WORTHING
University of Pittsburgh
Pittsburgh, Pennsylvania

THE OPTICAL SOCIETY OF AMERICA was organized in 1916 "*to increase and diffuse the knowledge of optics in all its branches, pure and applied, to promote the mutual interests of investigators of optical problems, of designers, manufacturers and users of optical instruments and apparatus of all kinds, and to encourage cooperation among them.*" It aims to serve the interests of all who are engaged in any branch of optics from fundamental research to the manufacture of optical goods.

### MEMBERSHIP

*Regular Members:* "Any person who has contributed materially to the advancement of optics is eligible for regular membership."

*Associate Members:* "Any person who is interested in optics is eligible for associate membership."

*Corporate Members:* "Any corporation desirous of encouraging the work of the Society is eligible for corporation membership."

The Society cordially invites to membership all who are interested in any branch of optics, either in research, in instruction, in optical or illuminating engineering, in the manufacture and distribution of optical goods of all kinds, or in physiological and medical optics.

### ANNUAL DUES

Regular members, $7.50; Associate members, $5.00; Corporate members, $50.00. These dues include subscription to the Society's official journal, the Journal of the Optical Society of America.

### MEETINGS

The Society holds two meetings per year: An annual meeting in the autumn, and a midwinter meeting jointly with the American Physical Society.

---

For further information concerning the Optical Society of America address the Secretary, Dr. L. B. Tuckerman, Bureau of Standards, Washington, D. C.

## ROCHESTER, NEW YORK SECTION OF THE OPTICAL SOCIETY OF AMERICA

C. E. BAHN, *President*
MRS. H. G. KINGSLAKE, *Secretary*

WALTER CLARK, *Vice-President*
A. A. LEVINE, *Treasurer*

*Councilors:* GUSTAVE FASSIN, OTTO SANDVIK, C. J. STAUD, T. R. WILKINS

Journal of the
OPTICAL SOCIETY
of AMERICA

VOLUME 23 AUGUST, 1933 NUMBER 8

# Studies in Refractive Index. III.[1]

A. M. TAYLOR AND DOROTHY A. DURFEE, *Institute of Applied Optics, University of Rochester*

(Received May 29, 1933)

In this paper experiments are described which indicate by direct interferometric measurements the distance of penetration of light into the second medium at total reflection. The intensity of the superficial wave is greater in the case when the electric vector of the incident light is in the plane of incidence than when it is perpendicular to this plane, as is required by theory. A method of multiple reflection was devised whereby the reflection coefficients in the two cases could be photometrically compared when the second medium is absorbing. The absorption coefficient and the refractive index of the liquid were measured in layers of the order of $10^{-3}$ cm thick and the values compared with the values deduced from the theoretical equations for the reflection coefficients. The results indicate that, for a saturated aqueous solution of potassium permanganate, the solvent is preferentially adsorbed at the surface, giving rise to smaller absorption of the superficial wave than would be expected from measurements of the absorption coefficient in the bulk.

## PENETRATION OF THE SUPERFICIAL WAVE AT TOTAL REFLECTION; AND OPTICAL EVIDENCE FOR THE EXISTENCE OF ADSORBED SURFACE LAYERS

### Introduction

The methods described in Part I of this series for the measurement of the refractive indices of liquids are all concerned in some manner with the critical angle. The double refraction of surface layers of some organic liquids has been observed and will be described in Part IV. But before confidence could be placed in such an extension of the methods, it was necessary to study the conditions of reflection of light polarized in and perpendicularly to the plane of incidence, particularly for angles slightly exceeding the critical angle. The purpose of the present paper is to verify the theoretical laws of reflection for liquids possessing strong absorption, i.e., having a complex refractive index; and to analyze the reasons for any discrepancies observed. These are explained in terms of the presence of adsorbed surface layers.

### Direct observation of the superficial wave

It is known that when light is reflected at an interface between one medium and another less dense, at angles greater than the critical angle, there is a superficial wave in the second medium. The intensity of this wave is different according as the incident light is polarized in or perpendicularly to the plane of incidence.[2] In either case it falls off rapidly as an exponential function of the distance from the surface. Raman observed that the light scattered from an obstacle, such as the edge of a razor blade, in the path of the superficial

[1] Parts I and II: A. M. Taylor and A. M. Glover, J. O. S. A. 23, 206 (1933).

[2] C. V. Raman, Trans. Opt. Soc. 28, 149 (1927).



BOSTON UNIVERSITY
COLLEGE OF LIBERAL ARTS
LIBRARY

wave, was strongly polarized in such a direction that the electric vector was perpendicular to the interface; i.e., in the plane of incidence. This, however, is not conclusive since ordinary unpolarized light when scattered by a metallic edge should theoretically be partially plane-polarized.

Consequently a modification of Raman's method of observation was used. A right-angled 45° prism of crown glass was mounted on an interferometer carriage behind the Michelson mirror in such a way that motion of the screw caused the hypotenuse face to approach a razor blade edge. The blade was normal to the face and was mounted at one end of one of a pair of thin steel strips 20 cm long, which were spot-welded together at their other ends. The slightest motion of the blade caused the welded ends of the strips to move in an arc. Increased magnification was obtained by causing the welded end to bear against a small galvanometer mirror suspended by a fiber under tension. Contact between the face of the prism and the edge of the blade was instantly recorded by a movement of a spot of light reflected from the mirror on to a distant scale. The mechanical magnification was such that after contact was established motion of the interferometer carriage through one wave-length of green mercury light (5461A) caused the spot of light to move through one centimeter on the scale.

Collimated light from a carbon arc was polarized by a nicol prism and was then internally reflected from the hypotenuse face of the prism at an angle slightly greater than the critical angle. The edge of the blade was observed in a microscope with a 32 mm objective, and the interferometer carriage was advanced slowly until the first sign of illumination of the edge was seen. The carriage was then advanced still further, while a second observer counted the number of fringes of green mercury light which passed a mark on one of the interferometer mirrors. At the first sign of motion of the spot of light on the scale, the movement of the carriage was stopped and the total number of fringes passed was recorded. This gave the maximum distance from the surface of the prism at which the superficial wave could be just detected.

The limiting distance at which the razor blade edge was illuminated by scattering from the superficial wave was found to be greater when the incident light was polarized with the electric vector in the plane of incidence than when the electric vector was perpendicular to this plane (see Table I). This confirms Raman's results.

TABLE I. *The mean value of four readings for an arbitrary angle of incidence slightly greater than critical.*

| Electric Vector | Fringes |
|---|---|
| $\perp$ to plane of incidence | 4.3 |
| $\parallel$ to plane of incidence | 7.5 |

The superficial wave has an amplitude given by

$$E_2 \exp\left[-2\pi(n_1 \sin^2\theta_1 - n_2^2)^{\frac{1}{2}}/\lambda\right],$$

where $\theta_1$ is the angle of incidence and $n_1$ and $n_2$ are the refractive indices of the first and second media, respectively. But for equal incident amplitudes $E_{1s}$ and $E_{1p}$, perpendicular and parallel respectively to the plane of incidence, $E_{2s}/E_{2p} = n_2/n_1$, and the intensities of the superficial wave in the two cases are therefore in the ratio of the squares of the refractive indices. The experiment confirms this result qualitatively, but because of the difficulty of controlling the angle of incidence $\theta$, quantitative results are not easily obtained.

**Absorption of the superficial wave**

If the second medium has a large coefficient of absorption the superficial wave will suffer more attenuation than is given by the exponential expression above. Moreover, this loss will be proportional to the intensity of the wave, i.e., it should be greater for light polarized with the electric vector in the plane of incidence than perpendicular to this plane.

For the purpose of observing this effect a saturated aqueous solution of potassium permanganate was used as the absorbing medium. The dispersion of this solution is known[1] but for the present purpose it was essential to measure the absolute value of the refractive index near wave-length 5450A and to measure the absorption coefficient directly without assuming the validity of the Beer-Lambert law. The measurements which were made will be described first.

*Refractive index.* In Part II the dispersion of a saturated aqueous solution of potassium permanganate was measured but absolute values of the refractive index proved hard to obtain with any accuracy. The curve could be trusted for relative rise or fall but not for absolute magnitude. This would have proved a serious handicap and an effort was made to fix one point on the dispersion curve absolutely. As a saturated solution of permanganate is very opaque to light of wave-length near 5450A, a method had to be devised which permitted of measurements with very thin films. The following plan was adopted.

Fringes were obtained in green mercury light ($\lambda = 5461$A) by interference of rays reflected from a flint glass plano-convex lens of radius of curvature of half a meter and a flint glass optical flat. The fringes were viewed in a travelling microscope having a 32 mm objective and vertical illuminator. The lens and flat were fixed together in a wooden clamp to prevent movement. The central dark spot of the Newton's ring system was then comparatively large because of deformation of the surfaces at the point of contact. The room temperature was 23°C. The cross wires of the eyepiece were then set accurately upon the thirtieth dark fringe, and at this point therefore the thickness of the air film was exactly $15\lambda$. Aqueous potassium permanganate solution saturated at 23°C was then run in between the lens and the flat, and the order of interference within the film redetermined by counting the fringes between the cross wires and the point of contact. From seven observations this order was found to be $40.5 \pm 0.1$, whence the refractive index of the solution is $1.350 \pm 0.003$. Near the 50th fringe the interference pattern disappeared because of absorption by the permanganate so that no greater accuracy could be obtained by increasing the thickness of the film.

This fixes the value of the refractive index at 5461A and while it does not invalidate the dispersion curve given earlier,[1] it indicates that the magnitude of the refractive index recorded there is too low.

*Absorption coefficient.* The absorption coefficient of a dilute solution of potassium permanganate was measured at 5450A. It was found necessary to redistil, from alkaline potassium permanganate, the laboratory supply of distilled water before consistent results could be obtained. A solution of $KMnO_4$, saturated at 23°C, was diluted to $2 \times 10^{-4}$ of its original concentration and was then found to have an optical density of 2.16 in a 10 cm column. From this it may be calculated that if the Beer-Lambert law holds, the absorption coefficient $n_{2\kappa}$ of a saturated solution should be $1.08 \times 10^{-2}$.

That this was exactly true was doubtful and a method was devised for measuring directly the absorption coefficient of a saturated solution. A spectrophotometer of the König-Martens type was set vertically. Two optical flats were "half-silvered" with a deposit of moderate density. Part of the silver was then removed and the plates put together with one drop of saturated permanganate solution between the clear parts. The plates were separated by three small spacers of metal foil about 20 microns thick, cut from adjacent portions of foil. Under these circumstances the plates were parallel to one another, and sharp straight fringes parallel to the slit of the spectroscope appeared in the spectrum of the light transmitted through the half-silvered portions.

The optical density of the film of permanganate solution was measured in the usual way with the spectrophotometer. The plates were then moved so that the light passed through the half-silvered portion and the wave-lengths of the narrow bright fringes in the spectrum were recorded. The wave-length drum of the spectrometer was previously checked against known spectrum lines and found without error appreciable for this purpose. Forty fringes were measured, and the thickness $z$ of the film determined from the usual formula $z = (m_2 - m_1)/2(\nu_1 - \nu_2)$ where $\nu$ is the wave number and $m$ the ordinal number of any fringe. From the figures in Table II

TABLE II.

| Ordinal number of fringe $m$ | Wave-length $\lambda$ | Wave number $\nu$ | Difference |
|---|---|---|---|
| 0 | 6908A | 14,474 $cm^{-1}$ | |
| | | | 2266 |
| 10 | 5972 | 16,740 | |
| | | | 2260 |
| 20 | 5263 | 19,000 | |
| | | | 2250 |
| 30 | 4707 | 21,250 | |
| | | | 2250 |
| 40 | 4255 | 23,500 | |

the mean of the observations gives a value for $z = 22.16 \times 10^{-4} \pm 0.05 \times 10^{-4}$ cm. The absorption coefficient is given by the formula $D = (4\pi n_{2K} z \log_{10} e)/\lambda$ where $D$ is the optical density. Experiment showed that $D$ was $2.32 \pm 0.02$ whence $n_{2K} = 1.05 \times 10^{-2} \pm 0.01 \times 10^{-2}$.

*The reflection coefficient.* In order to demonstrate the absorption of the superficial wave, measurements were made of the reflection of light at a glass-liquid interface. A rhomb of glass of refractive index 1.6203 for light of wave-length 5450A was made with an angle of 61° 23′ and of such dimensions (9 mm thick, 3.5 cm high and 9.8 cm long) that eight reflections could be obtained within it at angles of incidence which were greater than the critical angle from glass to saturated solutions of potassium permanganate. The long sides were optically flat and parallel to 5″ of arc. Cells, open at the top, were made by cementing thin glass plates to these sides, spaced at the edges by strips of glass 1 mm thick. These cells were cleaned with chromic acid, washed out with running water for some minutes and filled, when in use, with aqueous potassium permanganate solution.

The apparatus is indicated in Fig. 1. White light from a frosted lamp bulb was focussed on to the slit of a collimator in front of which was a Wollaston prism and bi-prism $W$ similar to that used in a König-Martens photometer. This served to illuminate the two halves of the slit with light polarized in two directions at right angles. The system was adjusted so that the light was polarized either in or perpendicular to the plane of incidence on the rhomb $R$. The rhomb was mounted on a spectrometer table. The light was dispersed by the prism $P$ and entered the telescope $T$; the spectrum was viewed by an analyzing eyepiece $A$ containing a slit shutter and a nicol prism of which the orientation could be read on a scale divided into degrees. A camera could be substituted for the eyepiece.

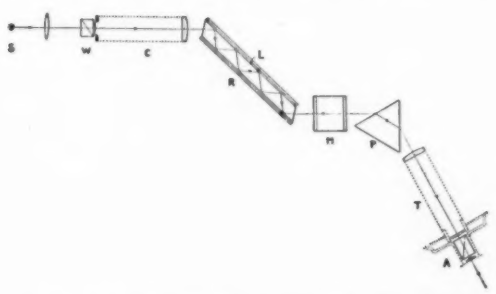


FIG. 1. $S$ is the source, $W$, Wollaston prism and bi-prism, $C$, collimator, $R$, rhomb, $L$, cells for liquid, $M$, compensating plate, $P$, prism, $T$, telescope, $A$, analyzing eyepiece. For convenience in drawing, the Wollaston prism, bi-prism and spectroscope slit are in elevation while the rest of the figure is in plan.

The plane parallel plate $M$ was of glass of the same refractive index as that of the prism $P$. Its purpose was to compensate for polarization produced by the prism and it was therefore set so that the angles of incidence of the light upon the plate and prism were the same, but the planes of incidence were mutually perpendicular. When this was done, the cells being empty, the two halves of the field were of equal intensity if the nicol was removed from the eyepiece $A$. The spectrum was divided into two halves by the image of the edge of the bi-prism. The polarizations in these two halves were mutually perpendicular and since the electric vector in either case was parallel or perpendicular to all planes of incidence in the system, no elliptical polarization was produced and by rotation of the analyzing nicol $A$, either field could be completely extinguished. Since the two halves of the field were of equal intensity in the absence of the nicol $A$, they were still of equal intensity when it was set with its principal plane at 45° to either direction of polarization of the two fields.

These conditions of equality of the two halves of the spectrum held when the cells of the rhomb were empty or filled with water or any transparent liquid, provided that the angle of incidence exceeded the critical angle. If, however, the cells were filled with any absorbing liquid, the absorption spectrum of the latter was evident in the reflected light. As the angle of incidence was increased, the superficial wave in the second medium was of less and less intensity and consequently less and less energy was subtracted from the reflected wave. However, as eight reflections occurred in the rhomb, the reflection coefficient was raised to the eighth power and the absorption spectrum could be observed in the reflected light for a considerable range. The two halves of the field were now no longer of equal brightness in

the region of absorption. The superficial wave, being of greater intensity when the electric vector was perpendicular to the surface, suffered greater energy loss than when the electric vector was parallel to the surface. Fig. 2 shows clearly the effect of greater absorption for the wave polarized with the electric vector perpendicular to the surface.

FIG. 2. Reflection spectra: (*s*) electric vector perpendicular to the plane of incidence, (*p*) parallel to the plane of incidence.

To make quantitative observations, the orientation of the rhomb was first found by means of a Gauss eyepiece. Then the rhomb was set at some convenient angle so that the incidence was greater than critical. The shutter in the eyepiece was so adjusted as to transmit only a portion of the spectrum centering about the absorption band at 5450A. The two halves of the field were then made of equal intensity by rotating the eyepiece nicol. The ratio of the intensities in the two halves of the field was equal to $\tan^2\phi$ where $\phi$ is the angle which the principal plane of the nicol made with the plane of polarization of the brighter half. Readings were made over a range extending from the critical angle to such an angle of incidence that the absorption bands had almost faded from the reflection spectra.

**Theory of the reflection coefficient**

The Fresnel formulae for reflection at an interface between two media of refractive index $n_1$ and $n_2'$ are

$$R_s = \sin^2(\theta_2-\theta_1)/\sin^2(\theta_2+\theta_1) \quad \text{and} \quad R_p = \tan^2(\theta_2-\theta_1)/\tan^2(\theta_2+\theta_1)$$

$$\text{or} \quad R_p/R_s = \cos^2(\theta_2+\theta_1)/\cos^2(\theta_2-\theta_1)$$

where $\theta$ is the angle of incidence in the first medium and $\theta_2$ the angle of refraction in the second, and $n_1 \sin\theta_1 = n_2' \sin\theta_2$. At the critical angle $\theta_2 = \pi/2$ and $\sin\theta_2 = 1$. Beyond that $\sin\theta_2 > 1$ and hence $\theta_2$ and $\cos\theta_2$ are imaginary. Now,

$$\cos\theta_2 = (1-\sin^2\theta_2)^{\frac{1}{2}} = (n_2'^2 - n_1^2\sin^2\theta_1)^{\frac{1}{2}}/n_2'$$

and in the case of an absorbing medium the refractive index is complex and $n_2' = n_2(1-i\kappa)$, where $i$ is the square root of minus one. So that

$$n_2'\cos\theta_2 = \{n_2^2(1-\kappa^2) - n_1^2\sin^2\theta_1 - 2in_2^2\kappa\}^{\frac{1}{2}}.$$

On expansion

$$R_p/R_s = [(\cos\theta_2\cos\theta_1 - \sin\theta_2\sin\theta_1)/(\cos\theta_2\cos\theta_1 + \sin\theta_2\sin\theta_1)]^2$$

and on substitution of the expression for $\cos\theta_2$ it follows that

$$R_p/R_s = [\{(a+ib)^{\frac{1}{2}} - c\}/\{(a+ib)^{\frac{1}{2}} + c\}]^2$$

where $c$ is written for $n_1 \sin\theta_1 \tan\theta_1$ and

$$a+ib = \{n_2^2(1-\kappa^2) - n_1^2\sin^2\theta_1 - 2in_2^2\kappa\}.$$

If $(a+ib)^{\frac{1}{2}} = x+iy$, then it may be seen that the absolute magnitude

$$|R_p/R_s| = (x^2+y^2+c^2-2xc)/(x^2+y^2+c^2+2xc)$$

where

$$x^2+y^2 = (a^2+b^2)^{\frac{1}{2}} \text{ and } 2x^2 = (a^2+b^2)^{\frac{1}{2}} - a.$$

The ratio $|R_p/R_s|$ has been observed experimentally and the results must now be compared with the

theoretical values. It might appear to be possible to reduce the expression for $|R_p/R_s|$ by suitable means, but a trial showed that over the range of experimental observations no satisfactory approximation could be made. Actually the computation of $|R_p/R_s|$ is tedious but not unduly so.

**Comparison with experiment**

The experimental readings of the angle of incidence of the light upon the rhomb could be converted into values of $\theta$, the angle of incidence of the light upon the glass-liquid interface. The magnitude of $R_p/R_s$ could then be computed for each value of $\theta$. As eight reflections occurred within the rhomb, the experimentally observed quantity was $(R_p/R_s)^8$ which is equal to $\tan^2\phi$ where $\phi$ is the angular setting of the analyzing eyepiece. $\mathrm{Tan}^2\,\phi$ was accordingly plotted against calculated values of $(R_p/R_s)^8$. The calculations of this latter quantity involved a knowledge of $n_2$ and $n_{2K}$. The graph obtained, although it was a straight line, did not pass through the origin and did not slope at exactly 45° as it should have done. It was found, however, that adjustment of $n_2$ caused the straight line to change its slope, while alteration of $n_{2K}$ tended to move the line parallel to itself. It was thus possible by a series of trials to establish a unique solution for the values of $n_2$ and $n_{2K}$ which would cause the straight line both to pass through the origin and to slope at 45°. This made the reflection coefficient as calculated equal to that observed. The graph is shown in Fig. 3. No other combination of values of $n_2$ and

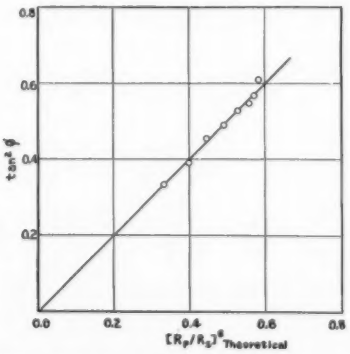


FIG. 3. Graph of the observed values of the reflection coefficient plotted against the calculated values.

$n_{2K}$ would achieve a similar result. The relation between the reflection coefficient, calculated from the formula, and the angle of incidence $\theta$ is shown by the curve in Fig. 4, while the observed values ($= \tan^2\phi$) are indicated by dots. The agreement is seen to be good. The values of $n_2$ and $n_{2K}$ thus found are

$$n_2 = 1.3505; \qquad n_{2K} = 0.93 \times 10^{-2}.$$

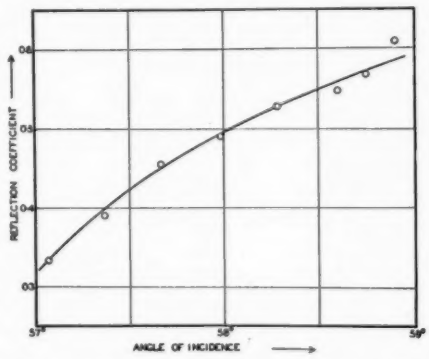


FIG. 4. Variation of the reflection coefficient with angle of incidence. The curve shows the calculated variation while the dots show the experimentally observed values.

The graph in Fig. 3 is very sensitive to variation in $n_2$; a value of 1.3500 is too small while 1.3510 is too large. The error in the value $n_2 = 1.3505$ is estimated to be of the order of $\pm 2$ units in the fourth decimal place. It is satisfactory to note that the value agrees well with the refractive index 1.35 measured by interference fringes. The graph of Fig. 3 is not so sensitive to variations in $n_{2K}$; but it may be noted that $n_{2K} = 0.97 \times 10^{-2}$ is too large while $n_{2K} = 0.89 \times 10^{-2}$ is too small. The value $n_{2K} = 0.93 \times 10^{-2}$ is therefore trustworthy to about two units in the second significant figure.

**Conclusion**

The value of $n_{2K}$ found from measurement of the reflection coefficient is distinctly less than the value found by direct observation of the absorption in a thin film. This was found to be equal to $1.05 \times 10^{-2}$. The source of discrepancy is not likely to be in the theory of the reflection coefficient and it is well outside experimental error. It might possibly be due to the existence at the interface of transition layers of variable refractive

index. These might be either in the glass or in the liquid. But the existence of such surface layers, while introducing a marked and often large phase change in the reflected beam, introduces only negligible errors in the magnitude of the reflection coefficient.[3] The experimental condition that the light was polarized accurately either in or perpendicularly to the plane of incidence eliminated any effect due to phase changes on reflection.

The reason for the low value of $n_2\kappa$ found by the method of multiple reflection must be sought elsewhere than in the existence of transition layers of slightly varying index of refraction. The results indicate that the superficial wave suffers less absorption than would a wave travelling in the bulk of the liquid. That is to say, the superficial wave, which exists in the surface only for distances comparable with a wave-length of light, must be travelling in a layer of which the absorption coefficient is lower than that of the bulk of the liquid. It has been shown that in salt solutions the concentration of the salt at the free surface is very much less than in the interior.[4] This must then be the cause of the low value of the absorption obtained from the total reflection method. The interface between the glass and the liquid preferentially adsorbs the solvent and while the change in refractive index produced is negligible, the change in absorption of the superficial wave is appreciable. That this phenomenon can be observed by optical means, even though the thickness of the layer of pure water is supposed to be only a few Angstroms, is to be ascribed to the rapid falling off in amplitude of the superficial wave as the distance from the interface increases. It is in consequence of this that the comparatively thin layer of preferentially adsorbed solvent is able appreciably to affect the reflection coefficient; that this alteration can be observed is due to the multiplication produced by reflection within the rhomb which raises the reflection coefficient to the eighth power.

[3] Handbuch der Physik **20**, 226 (1928).

[4] A. K. Goard, J. Chem. Soc. **127**, 2451 (1925); W. D. Harkins and H. M. McLaughlin, J. Am. Chem. Soc. **47**, 2083 (1925); W. D. Harkins and E. C. Gilbert, J. Am. Chem. Soc. **48**, 604 (1926).

# Infrared Radiations from Small Particles

A. H. PFUND, *The Johns Hopkins University*

(Received April 24, 1933)

It has been shown that crystals whose particle-size is small in comparison with the wave-length absorb but do not reflect within the region of selective absorption. It is suggested that within this region a powder ought to reveal an emission maximum. This suggestion is put to experimental test which shows that powder-films of quartz, barium sulphate and potassium carbonate show pronounced emission maxima. The behavior of quartz-powder is shown to be quite the inverse of that of a polished quartz plate.

THE following is a continuation of the writer's work on the optical behavior of small, crystalline particles. It has already been shown[1] that if the spectral transmission of a film of small particles, such as fumed magnesium oxide, be studied, it is found that, in the visible spectrum, where particle size and wave-length are of the same order of magnitude, the film appears brilliantly white in consequence of regular reflection from each particle. Proceeding into the infrared, the wave-length becomes large in comparison with the particle-size and only Rayleigh scattering takes place. Since losses by scattering are feeble, the powder film becomes almost transparent. It has further been shown by the study of radiometric effects[2] that, while massive plates of quartz, calcite, etc., reflect metallically in certain regions of the infrared, they lose this property if the materials be reduced to fine powders. Under these conditions, the particles absorb intensely the radiations corresponding to their "Eigenfrequenzen" and hence become very "black." On the basis of this work it was anticipated[3] that if these particles were heated, they would emit strongly in the region of selective absorption. Experiments dealing with this phase of the work are to be presented.

## APPARATUS

The essentials of the apparatus are shown in Fig. 1. A ground and polished plate of rocksalt $R(1\times8\times15\text{mm})$, after having been coated with a powder-film, was mounted in the center of a short, nichrome-wound furnace $F$. The radiations from the powder-film proceeded to a concave-mirror $M$ which formed an image of $R$ on the slit $T$ of the spectrometer. The latter was supplied with concave mirrors of 40 cm focal length and with a single rocksalt prism on a Wadsworth mounting. Because of the feebleness of the radiations from the powder-films, both spectrometer slits were widened to 0.9 mm. Measurements were carried out with the usual single-junction vacuum thermopile and D'Arsonval galvanometer. Careful tests showed that, because of the large angular opening of the furnace, no measurable radiations reached the spectrometer slit even when the empty furnace was red hot. Since the powder-film was heated largely by convection and radiation it was necessary to determine surface temperatures with a Pt–Pt Rh thermocouple made of fine wires 0.1 mm in diameter. One turn of these wires was wound around the middle of the rocksalt plate, the junction itself touching the powder-film at its center. These adjustments of furnace temperature were, of course, carried out on a dummy plate and powder-film. Since it was

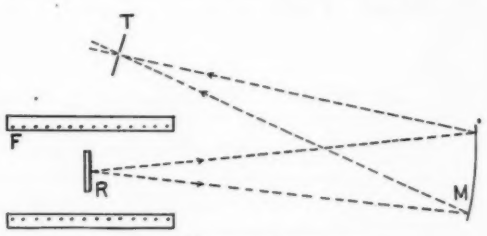


FIG. 1. Diagram of apparatus.

[1] A. H. Pfund, Phys. Rev. 36, 71 (1930).
[2] A. H. Pfund and S. Silverman, Phys. Rev. 39, 64 (1932).
[3] Pfund and Silverman, reference 2, p. 71.

necessary also, to obtain the radiations from a black body at the temperature of the powder-film, some sheet copper was bent into a cylinder 2 cm high and 1 cm in diameter. Both ends were closed and a central, vertical slot $1 \times 10$ mm was cut into the cylinder. This CuO black body was then mounted at the center of the furnace so that the image of the slot was formed on the spectrometer-slit $T$. The thermocouple made it possible to establish and maintain the temperature of 627°C (900°K) at which all measurements were carried out.

## Results

Most of the work was done on commercial powdered crystalline quartz.* Since the original particle diameter ($2.5\mu$) was too great, some of the material was shaken up with water, the coarser particles being allowed to settle out for 15 minutes. The milky fluid was then poured into a large flat dish and the water was allowed to evaporate. Microscopic examination showed that the average particle diameter had been reduced to $1.35\mu$. Especially prepared $BaSO_4$ (Blanc Fixe) was found to have a particle diameter of $1\mu$, hence no further comminution was necessary. To apply a powder film to the polished rocksalt plate the powder was first placed on a sheet of ground glass and was then thoroughly dispersed in butyl alcohol with a glass muller. Some of the resulting paste was then applied to the rocksalt plate and was spread back and forth with a glass rod about 4 mm in diameter. By timing the last stroke properly a film of remarkable uniformity was obtained. It was not difficult to produce films consisting of but a single layer of particles. When, in the following, films are designated as "thin" it is to be understood that the filament of a tungsten lamp can be seen readily through the film; a "medium" film transmits a barely recognizable image of the filament, whereas a "thick" film yields no visible image.

Since the powder-film is white for visible and near infrared radiations, pronounced reflections from furnace walls will take place. Upon coating the end of a massive brass bar with quartz powder and inserting this momentarily into the furnace (but out of contact with the walls) it was found that the energy reflected from the cold powder film, while large for the shorter wave-lengths, was negligible for wave-lengths greater than $5\mu$.

In Fig. 2 a number of curves for thin films are shown. The potassium carbonate film was applied as described; however, upon heating it did not turn white but seemed to disappear. Examination under the microscope showed that, in consequence of atmospheric moisture taken up during the process of mulling, the mixture had melted and formed a thin mottled film over the rocksalt surface.

These curves show the relation between the emissive power (i.e., ratio of emission from powder to that of the black body, both at a temperature of 900°K) and temperature. It is seen that marked emission maxima occur at wave-lengths which are somewhat greater than those of the bands of selective reflection.[4] Since, as has been stated, fluffy powders seem to have lost the property of selective reflection, it is clear that the emission maxima must coincide more or less closely with the regions of maximum absorption. That this is true is shown by a comparison of these results on emission with the results on the radiometric effects (absorption).[5]

In order to determine the influence of film thickness on emission, three different quartz films, classified as very thin ($A$), medium ($B$) and very thick ($C$), were studied (see Fig. 3). The thinnest film was only one particle deep with blank areas between particles. This precludes any trapping of radiation by multiple reflections.

As might have been anticipated, these results show that, with increasing thickness of powder film, the bands of selective emission become higher and broader. Having found selective emission for a film of potassium carbonate, it was decided to investigate the emissive-power of a film of Pyrex glass. A large bulb was blown from which an area of sensibly constant thickness, as determined by means of the channeled spectrum, was cut out. The film, which had a thickness of

* Known as Tamm's Velveteen Silica.

[4] Schaefer and Matossi, *Das Ultrarote Spectrum*, p. 343, (1930).

[5] Pfund and Silverman, reference 2. While it is true that the radiometric effects were obtained with unheated powders, it is to be borne in mind that, for crystalline materials, a rise in temperature produces only a small shift in the positions of reflection (and, probably) absorption maxima. See H. Rubens und Hertz, Berl. Ber., p. 256 (1908); A. H. Pfund, J. O. S. A. 15, 71 (1927).

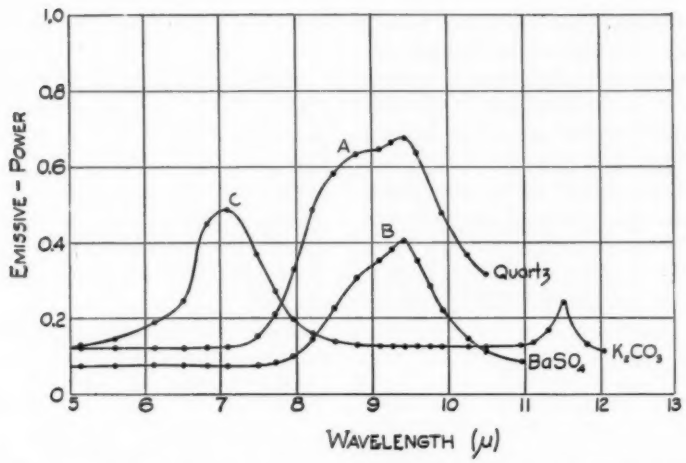


FIG. 2. Emissive powers of powder-films at 900°K, (*A*) quartz, (*B*) barium sulphate, (*C*) potassium carbonate.

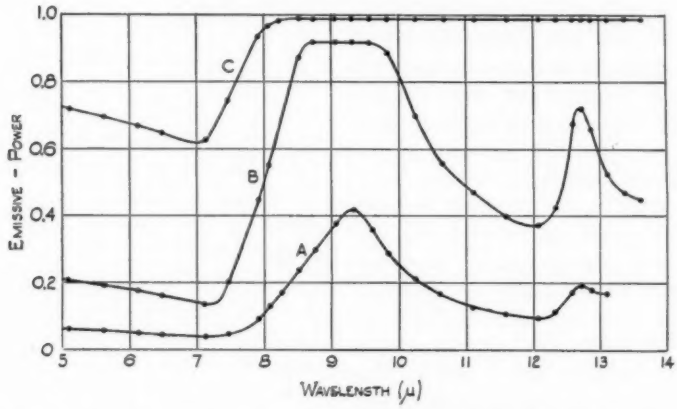


FIG. 3. Emissive powers of quartz powder-films, (*A*) thin, (*B*) medium, (*C*) thick.

2.10 microns was mounted in the furnace and heated to 900°K. The results are shown in Fig. 4. From this it is evident that thin films have high emissive powers in regions of strong absorption (9$\mu$), whereas in the region of transparency (2$\mu$) the emissive power is low.

The question arose (after the apparatus had, unfortunately, been dismantled) as to whether there was a suitable film-thickness which would yield an emission greater than that of a massive plate. That this must be the case is evident. It was settled, however, by studying the transmission, reflection and absorption of a wedge-film of silver, ranging in thickness from zero to the thickness of maximum reflecting power. A maximum of absorption of 60 percent of green light was found for a film-thickness yielding 28 percent reflection. Since a massive silver plate whose reflecting power is 92 percent can absorb no more than 8 percent of green light, it is evident that the radiant emission from the heated film must be much the greater.

## DISCUSSION

Rayleigh's law of scattering may be stated in the following simple form:

$$I_s = I_0 K(d^6/\lambda^4)$$

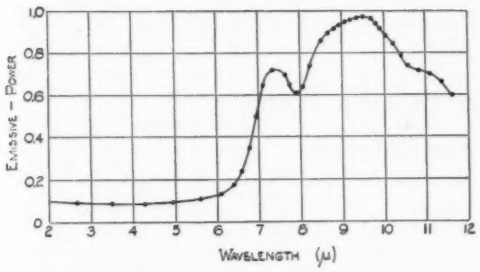


FIG. 4. Emissive power of flake of Pyrex glass.

where $I_s$ = the intensity of the scattered light; $I_0$ = the intensity of the incident light; $K$ = a constant; $d$ = diameter of the scattering particle; $\lambda$ = the wave-length of the incident light.

If, therefore, transparent particles for which the ratio $d/\lambda$ is small be studied, it is evident that the scattered light will be weak and that, in consequence, copious transmission will result. Applying this law to regions of absorption it may be anticipated that here, also, scattering will be feeble. In consequence the incident radiation is weakened by true absorption alone, the powder-film in question becoming black. In accordance with Kirchhoff's law a heated powder-film ought, then, to emit most strongly in those spectral regions for which the absorption is greatest.

These considerations are quite in accord with the experiments previously presented. The interesting result follows that, while a massive mirror of quartz shows minima of emission in the region of selective reflection, a fluffy quartz powder shows maxima of emission in the closely adjacent regions of maximum extinction coefficient. These results are set forth in Fig. 5 where curve $A$, for the emission of a heated plate of quartz, has been calculated from the data given in Rosenthal's paper.[6]

In order that strong absorption may take place in a powder-film, it is further necessary that the particles be loosely packed. These considerations may be illustrated by the absorbing and reflecting properties of bismuth black.[7] If the powder forming an initially black layer be collected in a pile and be subjected to intense pressure between

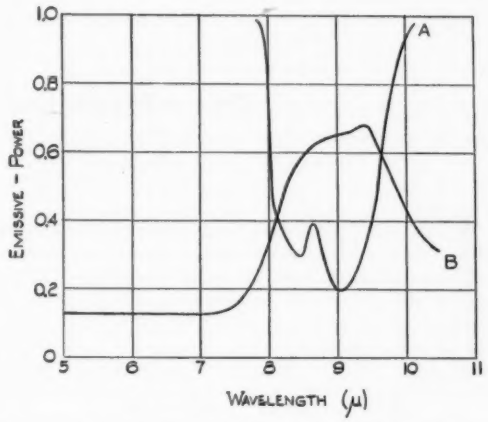


FIG. 5. Emissive powers: ($A$) Rosenthal's curve for a polished quartz plate, ($B$) quartz powder-film.

two pieces of plate glass, a highly reflecting, metallic surface is created. It appears not improbable that soot, bismuth black and platinum black owe their blackness not to a "trapping" of radiation by multiple reflections but to the virtual absence of reflection found in loosely packed films made up of minute absorbing particles.

Incidentally it may be remarked that recently, while distilling tellurium in an evacuated tube of Pyrex glass, it was found that while a brilliant mirror-like deposit appeared at some distance from the heated bit of tellurium, an intensely black coating was thrown down a few centimeters away. Upon shattering the glass tube and viewing normally a black fragment in light streaming over the shoulder, the surface appeared at its intensest black. By swinging the surface into a horizontal position so as to bring about a tangential illumination, the surface assumed a brilliantly white, velvety appearance. These changes are interpreted as being due to microscopic needles standing perpendicular to the surface of the glass tube. The white appearance indicated that light was being reflected from the sides of the needles whereas the intense black was accounted for on the assumption of true trapping by multiple reflections. Subsequent microscopic examination revealed the existence of a needle-like formation very clearly. Micrometer measurements showed that the needles were 0.015 mm high.

[6] H. Rosenthal, Ann. d. Physik **68**, 783 (1899).
[7] A. H. Pfund, reference 5.

# On the Astigmatism of the Concave Grating

G. H. DIEKE, *The Johns Hopkins University*

(Received April 24, 1933)

For light of any given wave-length, the angle of incidence on a concave grating which gives minimum astigmatism has been calculated from the general expression for the astigmatism. To obtain the maximum efficiency with a Paschen mounting, the use of two fixed slits is suggested. For the lower orders an angle of incidence of about 13° is suitable. The astigmatism in the ultraviolet is then not harmful for most purposes. It is shown that the Rowland mounting is very inefficient as far as intensity losses by astigmatism are concerned, whereas the Eagle mounting represents very nearly the optimum condition. A method is suggested to make use of the astigmatism for intensity measurements.

AS a rule the astigmatism of the concave grating is an inconvenience which one tries to eliminate as much as possible and it is essential therefore to know the conditions under which it can be reduced to a minimum. As far as I know there is in the literature no discussion of the astigmatism in the general case. Only special cases for the Rowland mounting of the concave grating and for the Eagle mounting were treated. But as in recent years the so-called Paschen mounting is used more and more by spectroscopists, it is of interest to investigate the astigmatism in this case also. I know of several big grating spectrographs for which the astigmatism is unnecessarily large and where it could easily be reduced by a factor five or six by a suitable disposition of the slit. I hope, therefore, that the following discussion will be of some use to those contemplating the construction of a grating spectrograph.

To secure the best definition of a spectral line, it is necessary that slit, grating and photographic plate be on the Rowland circle (Fig. 1). If the incident light makes an angle $\alpha$ with the normal and the diffracted beam emerges under an angle $\beta$ we have

$$\sin\alpha + \sin\beta = n\lambda/d, \qquad (1)$$

in which $\lambda$ is the wave-length, $n$ the order and $d$ the distance between two successive rulings on the grating. For the purpose of this paper it is entirely immaterial whether we are in the first, second or any other order, as the astigmatism is completely determined by the angles $\alpha$ and $\beta$ and therefore with a given grating by one of the angles and the product $n\lambda$. We shall give, therefore, all wave-lengths as if we were in the first order, $\lambda = 24{,}000$A meaning the place at which the first order of 24,000 would be observed, the second order of 12,000A, third of 8000A, etc. All results can be so stated as to be valid for any concave grating, if instead of the wave-length we use $g = \lambda/d$ as parameter. In order to make the results more directly applicable to the most commonly used gratings, I shall use in this paper the wave-length for a grating with 15,000 lines per inch. For a grating with $p$ lines per inch $\lambda$ will have to be replaced by $15{,}000\lambda/p$ in order to get the correct wave-length for the grating.

It might be useful to state here the character-

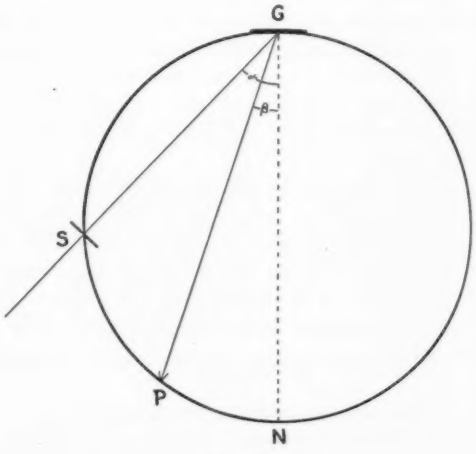


FIG. 1.

istics of the principal mountings which are in common use.

(A) Paschen mounting: $\alpha$ fixed, $\beta$ arbitrary, slit, plateholder and grating fixed.
(B) Rowland mounting: $\alpha$ variable, $\beta=0$, slit fixed, grating and plateholder moving.
(C) Abney mounting: $\alpha$ variable, $\beta=0$, plateholder and grating fixed, slit moving.
(D) Eagle mounting: $\alpha=\beta$, slit fixed, grating and plateholder moving.

Each one of these mountings has its advantages and disadvantages. Whereas in the early work the Rowland mounting (or the Abney mounting which is only a variant of it) was preferred because it gave the spectrum on the normal of the grating where the dispersion is constant, a useful feature in wave-length determination but one which became of less importance after a good system of wave-length standards had been established and the most accurate wave-length determination was no longer the only purpose of the use of a grating spectrograph.

For that reason the Paschen mounting, with its convenience in having no moving parts requiring adjustment, became more and more popular. An additional very great advantage is the fact that the whole spectrum in all orders can be photographed in one exposure. The astigmatism, however, is in many cases a serious drawback.[1] Various devices have been designed[2] to eliminate it completely. These work very well when used properly but involve the use of mirrors or lenses with delicate adjustments and complicate the use of the mounting considerably. One of the essential advantages of the Paschen mounting, that it is always ready for use without any adjustment, is then lost.

For many purposes it is unnecessary to correct the astigmatism completely as a small amount does no harm. One of the purposes of this paper is to show how the spectrograph must be constructed if we wish to keep the astigmatism as small as possible.

If only a point of the slit is illuminated it produces, on account of the astigmatism, a spectral line of length[3]

$$\zeta l = (\sin^2\beta + \sin\alpha \operatorname{tg}\alpha \cos\beta) l, \qquad (2)$$

in which $\alpha$ and $\beta$ are the angles which the incident and emergent light beam make with the normal of the grating. $l$ is the length of the ruling.

(2) gives the astigmatism $\zeta$ of a grating with rulings of unit length as function of the two variables $\alpha$ and $\beta$. On account of (1) we can regard it also as a function of $\alpha$ and $\lambda$. We see that for a given angle of incidence $\alpha$ the astigmatism is smallest on the normal of the grating where $\beta=0$. It increases symmetrically on both sides. $\zeta$ becomes infinite for $\alpha=90°$ and one for $\beta=90°$.

For a given wave-length $\zeta$ is a function of $\alpha$ alone. For each value of $\lambda$ there must be one $\alpha$, for which the astigmatism is a minimum and the value of $\zeta$ for this $\alpha$ represents the minimum astigmatism for this wave-length which can be obtained with the grating under any condition.

The condition that (2) be a minimum for constant $\lambda$ gives

$$\begin{aligned} &g^3(4-3x^2+3x^4-3x^6) \\ &\quad +g^2(-16x+28x^3-26x^5+10x^7) \\ &\quad +g(-4+28x^2-39x^4+30x^6-11x) \\ &\quad +8x-20x^3+20x^5-12x^7+4x^9=0, \end{aligned} \qquad (3)$$

in which $x=\sin\alpha$ and $g=\lambda/d$. The solution of this equation can be found by an approximation method. The results are represented in Fig. 2*A*, *B* and Fig. 2*C* gives the minimum astigmatism as function of $\lambda$.

The situation is somewhat different for long and short wave-lengths and to bring this out in Fig. 3 the astigmatism is plotted as function of $\alpha$ for three typical wave-lengths. Fig. 3*C* is for $\lambda=5080$A ($g=0.2$). We see the deep minimum for $\alpha$ about 8° and an insignificant maximum at $\alpha=-40°$ (negative $\alpha$ means that $\alpha$ and $\beta$ are on opposite sides of the normal). The curve, Fig. 3*B*, is for $\lambda=20{,}320$A. This wave-length can be obtained only for a smaller range of $\alpha$'s according to (1). There is still a minimum but it is not as deep. The maximum at the left side of the curve is still existent, but so insignificant that it cannot be shown on the scale of the curve. Fig. 3*A* for which $\lambda=27{,}100$ shows that for such large values

[1] This applies, of course, to any grating mounting which does not use mirrors or lenses.

[2] Runge and Maunkoff, Zeits. f. Physik **45**, 13 (1927).

[3] Kayser, *Handbuch der Spektroskopie*, I, 463.

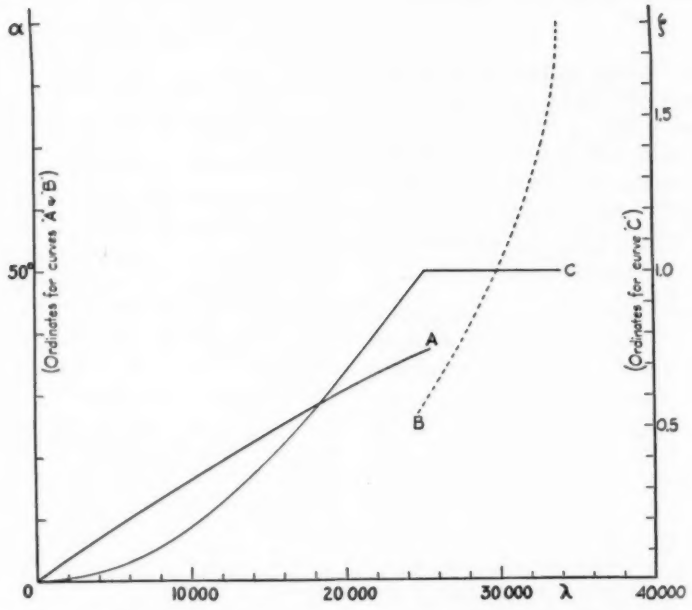


FIG. 2. *A*, *B*. The angle of incidence for minimum astigmatism; *C*, the minimum astigmatism as function of the wave-length (grating with 15,000 lines per inch).

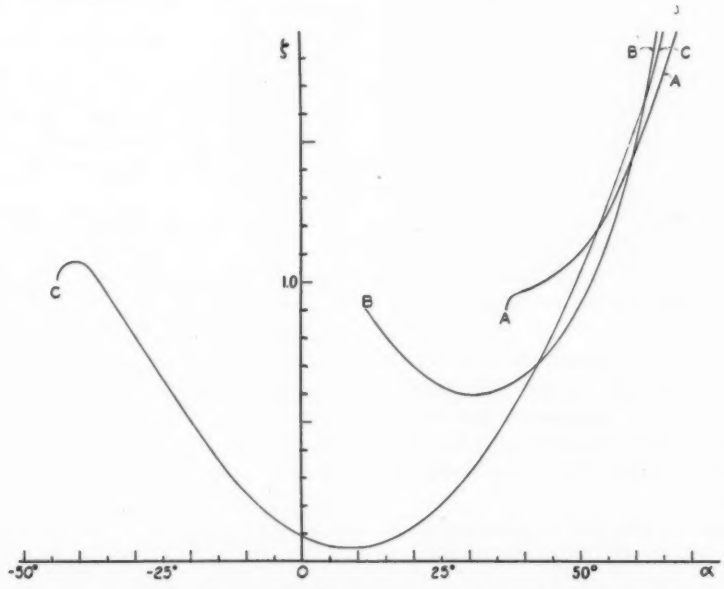


FIG. 3. *A*, astigmatism for λ=27,100A as function of the angle of incidence; *B*, the same for λ=20,320A; *C*, the same for λ=5080A.

of $\lambda$ there is no maximum or minimum. The minimum astigmatism in this case is obtained if $\alpha$ is as small as possible, which means that the emergent light beam is nearly tangent to the grating surface, ($\beta = 90°$).

The difference between the curves, Fig. 3*A* and Fig. 3*B*, explains the break which occurs in Figs. 2 and 3 for about $\lambda = 25{,}300$. Below this wave-length the astigmatism as a function of $\alpha\lambda$ is represented by a curve of the type of Fig. 3*B*. With increasing wave-lengths the minimum becomes more shallow and the value of $\zeta$ at the minimum approaches one and even exceeds it a little. If we go to still larger wave-lengths the minimum disappears completely and we have a curve like Fig. 3*A*. The astigmatism has then its smallest value $\zeta = 1$ for $\beta = 90°$, i.e., for grazing emergence of the light. The value of $\alpha$ for which we have grazing emergence and therefore the smallest astigmatism is given by the dotted line in Fig. 2. With it corresponds the horizontal part of Fig. 2*C*.

## Application to Grating Mountings

One point which is held essential for a grating mounting is that longer wave-lengths i.e., high orders of the visible and ultraviolet, can be obtained because the dispersion and resolving power is then very high. This necessitates a rather large value of $\alpha$ but the figures show that for the small wave-lengths the astigmatism is now unnecessarily large.

There is, of course, no way of securing with one fixed slit, at the same time, a small amount of astigmatism and the possibility of obtaining high orders. How, in an individual case the slit ought to be placed, depends entirely on the circumstances, on the grating, e.g., whether it is good in the higher orders or not, on the amount of space available and also, of course, on the kind of investigation the spectrograph is chiefly meant for.

A small amount of astigmatism can be tolerated in most cases. Let us fix this amount somewhat arbitrarily to be $\zeta = 0.1$. For this value the total astigmatism $\zeta l$ of a grating with 5 cm long rulings is 5 mm. If the illuminated slit is longer than about 5 mm, there is no loss of intensity due to astigmatism in the central portion of the line.[4]

Now it is possible with any light source (except perhaps very narrow discharge tubes seen end on) to form a 5 mm long image on the slit and still fill the whole grating. Theoretically there is always the possibility of avoiding a loss of intensity due to astigmatism by using an illuminated slit longer than $\zeta l \cos\alpha/\cos\beta$. But apart from the fact that it would be often impossible to have an image of this size on the slit and still fill the grating with light, there is the fact that the definition of the line and resolving power of the grating diminishes considerably if too long a slit is used. But a slit length of 5 mm is in almost all cases not objectionable.

With an astigmatism of 0.1, two points on the slit which are farther than about 5 mm apart give two separate spectral lines. That is very often sufficient, e.g., to study the behavior of the light at the two electrodes in arcs and sparks.

Fig. 2*C* shows that it is possible to have $\zeta = 0.1$ only for $\lambda < 7600$A. From Fig. 2*A* we see that if the slit is so placed that the incident beam makes an angle $\alpha$ of about 13° with the normal $\zeta \leq 0.1$ for all $\lambda < 7600$. If $\alpha$ is either increased or decreased the effect is that the upper wave-length limit, for which $\zeta \leq 0.1$, becomes lower, so that we might say that $\alpha = 13°$ is about the most favorable angle of incidence for a Paschen mounting.

For this angle $\alpha = 13°$ the maximum wave-length which can be obtained for $\beta = 90°$ is about 20,600A, for $\beta = 45°$, $\lambda = 15{,}700$. As a rule it is not advisable to have too large values of $\beta$ and often this is entirely prohibited by the limitations of space and the construction of the spectrograph. The limitation which an angle of incidence of 13° puts on the higher orders is undesirable. The best way out is to use a second slit for which $\alpha$ is larger and use it mainly for the higher orders.

For the low wave-lengths this second slit would be less useful on account of its increased astigmatism but for the higher orders there is not much difference between the minimum astigmatism and the astigmatism obtained with a slit for which $\alpha$ is between 30 and 40 degrees.

[4] In order that the astigmatism cause no diminishing of the intensity, the illuminated slit must be at least $\zeta l \cos\alpha/\cos\beta$ long. Then the middle of the line has the same intensity as it would have if the image were stigmatic. The factor $\cos\alpha/\cos\beta$ differs only in extreme cases much from one.

Fig. 4*A* gives the astigmatism if $\alpha=13°$, Fig. 4*B* if $\alpha=38°$. It shows that for all wave-lengths below 16,000A the astigmatism is smaller for $\alpha=13°$ and very considerably smaller for short wave-lengths. The dotted curve gives the minimum astigmatism.

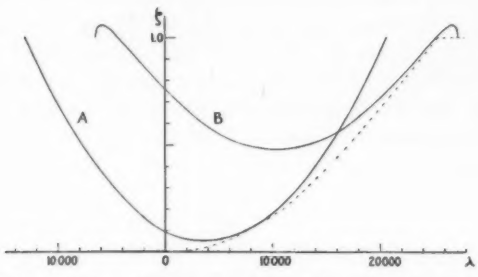


FIG. 4. Astigmatism as function of wave-length. *A* for $\alpha=13°$; *B*, for $\alpha=38°$.

A few details about such an arrangement for the Paschen mounting at The Johns Hopkins University will perhaps be useful. For the first slit $\alpha=16°$, for the second one $\alpha=38°$. The choice of these angles was determined principally by other reasons which have nothing to do with the astigmatism. One of the slits is installed first and the spectrograph focussed. This is done by placing grating and slit on the Rowland circle and adjusting the steel rails which serve as plateholder so that the best focus is obtained. For an ideal grating the rails must, of course, then also be exactly on the Rowland circle. For the grating which is used at present that is very nearly the case. But there are gratings which have a large error of run for which the rails are considerably off the Rowland circle, e.g., a grating employed in the same mounting previously showed deviations of the focal curve from the Rowland circle of more than 5 cm for some wave-lengths.

After the spectrograph has been focussed for the first slit no further adjustments are made of this slit, the grating, or the plateholder. The second slit, which should be constructed to fit between the plateholder rails is then put in place. With a perfect grating and the first slit exactly on the Rowland circle, the second slit should also be exactly on the Rowland circle but in practice it will usually be of little off. It should therefore be provided with a sliding tube and scale for reading its exact position. The correct position of the slit can then be found by taking focus plates leaving the plateholder unchanged and pushing the slit in and out. With our grating it was found that if the second slit was in focus for one wave-length it was very nearly so for all other wave-lengths. If this is not the case a different setting is required for different parts of the spectrum. But even in unfavorable cases a comparatively large part will be sharp simultaneously for one setting of the slit.

A small part of the plateholder in the immediate vicinity of the slit cannot be utilized. It would be possible to construct the spectrograph in such a way that this region would not be greater than about 1 mm, but other inconveniences would result in consequence. With the author's spectrograph the region screened off by the slit and its mounting is about 10 cm (for the slit at 13° and a grating of 15,000 lines per inch this dead region is at $\lambda=7620$A). If one is interested in just this region it can be obtained with somewhat increased astigmatism on the other side of the normal (compare Fig. 4) or if that cannot be obtained on account of limitations of space, the other slit must be used.

If, in photographing the spectrum, e.g., with the wide angle slit, one is interested in the region obscured by the other slit, it can be removed. To facilitate the removal and replacement, the following mounting was constructed. The slit tube is mounted on a heavy iron block (about $17\times12\times5.5$ cm), on the bottom of which three steel balls are soldered. These fit exactly into three holes of a brass base plate. After the slit has been lined up, the brass plate is cemented to the stone slab which carries the plateholder. The slit can now be removed when necessary in a few seconds and put back in exactly the same position. The weight of the iron block assures the necessary rigidity. The light source is outside of the grating room, a pipe leading from the wall to the slit protecting the plates from scattered light. The connection between the slit and the pipe is made by black cloth which prevents the transmission of vibrations of the pipe to the slit. It can be easily removed for inspection of the image of the light source on the slit.

The use of more than one slit with the Paschen mounting increases the usefulness of the spectro-

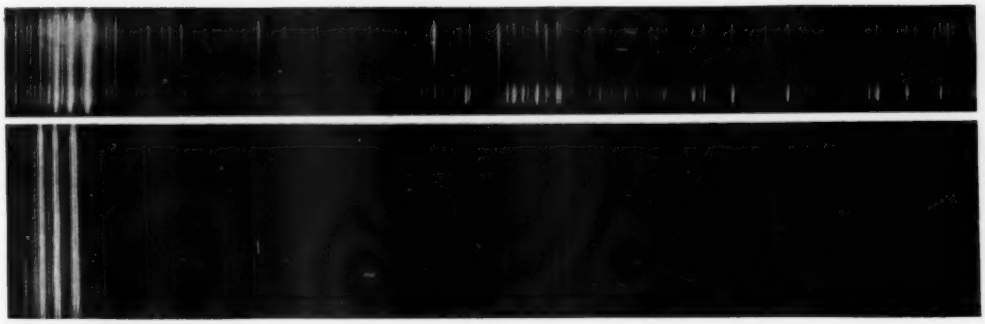

FIG. 5. Manganese spectrum near 2700 (natural size) above $\alpha=16°$, $\zeta=0.084$; below $\alpha=38°$, $\zeta=0.57$. The dispersion is slightly different in the two pictures.

FIG. 6. Hg 2537 (natural size); left $\alpha=38°$, $\zeta=0.58$; right $\alpha=16°$, $\zeta=0.083$.

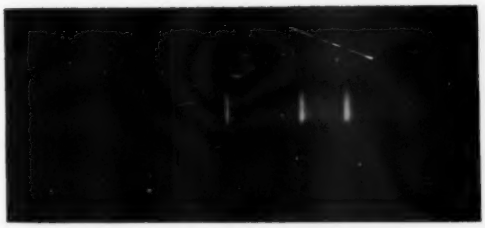

FIG. 7. $N_2$-bands at 2377A (natural size); left, $\alpha=38°$, $\zeta=0.56$; right, $\alpha=16°$, $\zeta=0.088$.

FIG. 8. Comparison spectra produced by diaphragm on slit (natural size); $\zeta=0.083$.

graph also in other respects. If complicated light sources are used much more time is usually spent in building them up and perfecting them than in taking the actual photographs. During all this time the place in front of the slit is occupied and other workers are prevented from using the spectrograph. From this point of view the spectrograph with two slits is equivalent almost to two complete spectrographs, and its usefulness almost doubled. I understand that, for this reason, the original Paschen mounting at the University of Tübingen has, for sometime, been provided with a second slit.

The Figs. 5–8 illustrate the results which can be obtained. Fig. 5 is a portion of the spectrum of the Mn arc at 2720A. The upper figure taken with the 16° slit allows one to recognize easily the lines which are produced only at the electrodes, whereas in the lower figure, taken with the 38° slit, this difference is unrecognizable on account of the larger astigmatism. The lines in the lower figure may look smoother and present a better appearance than those in the upper figure, but there is no doubt that the latter ones give much more valuable information about the character of the lines. Fig. 6 shows the 2537 Hg line and Fig. 7 some $N_2$ bands at 2977. In both figures the left side was taken with the 38° slit and the right with the 16° slit. Both exposures were made under as nearly identical circumstances as possible. The figures show the great loss of intensity due to the increased astigmatism. Fig. 8 shows that it is quite feasible to use a diaphragm on the slit to obtain a suitable comparison spectrum if the astigmatism is not too large.

### Astigmatism for the Rowland Mounting

As $\beta = 0$, the astigmatism becomes in this case

$$\zeta = \sin \alpha \operatorname{tg} \alpha; \qquad g = \lambda/d = \sin \alpha.$$

Fig. 9 shows that the astigmatism for the Rowland mounting is much larger than the minimum astigmatism for almost all wave-lengths. For large $\lambda$ the loss of light caused by this is so great that the usefulness of the Rowland mounting is greatly reduced.

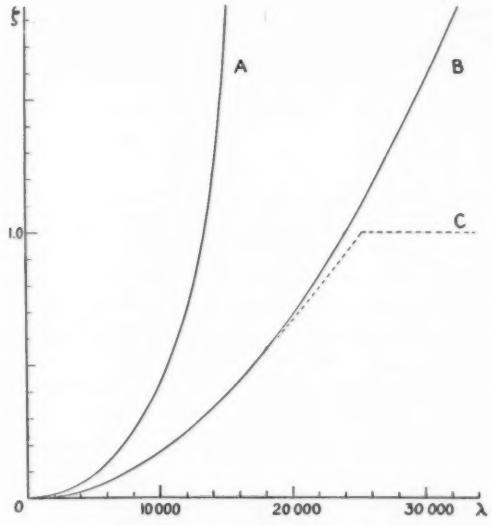


Fig. 9. Astigmatism as function of wave-length; *A*, for Rowland mounting, *B*, for Eagle mounting, *C*, minimum astigmatism.

### Eagle Mounting

In this case $\alpha = \beta$ and

$$\zeta = 2 \sin^2 \alpha; \qquad g = \lambda/d = 2 \sin \alpha.$$

Eagle[5] has pointed out that for his mounting the astigmatism is much less than with that employed by Rowland. This is brought out clearly in Fig. 9. But Fig. 9 shows also that the astigmatism for the Eagle mounting is only very little larger than the minimum astigmatism. In fact, for small wave-lengths the difference is insignificant and even at $\lambda = 24{,}000$A the difference is only about 8 percent. For still longer wave-lengths the difference increases but as only very few concave gratings permit to reach such long wave-lengths, this is of little practical importance.

Therefore the Eagle mounting satisfies the requirement for minimum astigmatism almost completely. It is in this respect far superior to the Rowland mounting[6] and for most wave-lengths slightly better than the Paschen mounting. The advantage of the latter is due to the fact that it has no adjustments and permits the photography of the whole spectrum in one exposure.

### Use of the Astigmatism for Intensity Measurements

Whereas for most purposes the astigmatism is an inconvenience, it is possible to use it with advantage for intensity measurements.

In all photographic intensity measurements of spectral lines a calibration of the photographic plate is required. In principle this amounts to finding out what blackening is produced by a series of light sources of known intensity ratios. The methods employed differ only in the manner in which this is done.

If we have a spectral line produced by an astigmatic grating spectrograph, a part of the middle of the line is of uniform intensity. Towards the ends the intensity falls off and the rate with which it decreases is determined by the astigmatism and therefore known. We can get, therefore, in any part of the spectrum calibration marks without any effort and without any auxiliary apparatus.

It would be premature to give here the details of how this can be used for photographic intensity measurements with concave gratings, before they are tested thoroughly experimentally. A necessary prerequisite is that the grating be of such a nature that every part along the rulings contributes evenly to the intensity of a line. Only in that case can the intensity distribution along the lines be so simple that it can be calculated easily.

This method of using the astigmatism for the calibration of photographic plates for intensity measurements has some obvious advantages. The

[5] A. Eagle, Astrophys. J. **31**, 120 (1910).

[6] If one wishes to use cylindrical lenses to correct the astigmatism the Rowland mounting has some advantages, as a larger part of the spectrum can be corrected simultaneously.

chief advantage is that its application is so simple. If the intensities of only a few lines in a narrow spectral range are to be compared and there are no objections to the use of a wide slit, all that is necessary is to photograph the spectrum and run the lines lengthwise through a microphotometer. Knowing the astigmatism which can be calculated very accurately from the formulae of this paper, one can then evaluate the intensities from the microphotometer curves.

If there are many lines, it will be more convenient to photograph the spectrum in the usual way with a narrow or moderately wide slit and take, on the same plate or a plate from the same box, a continuous spectrum. This procedure will always be necessary if the lines which are to be compared are far apart.

As the astigmatism can, without any serious difficulties, be varied within wide limits, this method of intensity measurements is very flexible and can easily be adapted to any problem.

I hope that it will be possible to report in the near future on experiments which are being carried out at present in this laboratory to test the practicability of this method.

I wish to thank Mr. Peter A. Cole for his help with the experimental test of the results of this paper.

# A Method of Projecting Star Images Having Coma and Astigmatism

R. KINGSLAKE AND A. B. SIMMONS, *Institute of Applied Optics, University of Rochester*

(Received May 13, 1933)

After a brief theoretical introduction, the procedure for plotting the sections of an imaging cone from a point source, for one single zone of a lens in the presence of one or more aberrations is explained. The process is much simplified by a convenient graphical construction. A method is then described for projecting the sections due to coma and astigmatism on a screen so that they may be shown to a class. Photographs are included in the paper which show how remarkably the projected sections agree with the theoretically computed figures.

## THEORETICAL INTRODUCTION

THE properties of the familiar aberration astigmatism are very well known, chiefly because a lens system having pure astigmatism can be readily constructed by superposing a weak cylinder lens on an achromatic lens. Coma, on the other hand, is by no means so familiar; for although most lenses have some coma for extra-axial object points, it is very unusual to find the coma entirely free from astigmatism. In fact, Gleichen[1] distinguishes two types of astigmatism, one as from a cylindric lens as mentioned above and the other from oblique passage through a single refracting surface. The latter "type" of astigmatism is really a mixture of coma and astigmatism, the second slanting focal line being really the "characteristic focal line" appropriate to this particular mixture, as described by Conrady.[2]

The properties of coma and astigmatism are best illustrated by calculating a series of cross sections of the cone from one single zone of the lens in the immediate neighborhood of the image of a point source.

The simplest approach to the theory of the primary, Seidel, or third order aberrations of a lens is undoubtedly by optical-path-difference[3] or eikonal[4] methods, which give the following equation for the path-difference between two quantities of light arriving at the ideal Lagrangian image-point in the paraxial image-plane, one having come *via* the center of the exit pupil, and the other having come via the point in the exit pupil having coordinates $(x, y)$:

$$OPD=(A/4l')(x^2+y^2)^2+(B/l')y(x^2+y^2)h+(C/2l')(x^2+3y^2)h^2+(D/2l')(x^2+y^2)h^2+(E/l')yh^3. \quad (1)$$

Here $l'$ is the distance of the final image from the exit pupil; $A$ is the aberration-coefficient of spherical aberration, $B$ of coma, $C$ of astigmatism, $D$ of curvature of field, and $E$ of distortion; $h$ is the height of the extra-axial image-point above the optical axis of the lens.

The optical-path-difference at any point in the exit pupil is the distance between the actual wave front and the ideal sphere centered about the Lagrangian image-point $L$ (Fig. 1). The "angular" aberration $\alpha$ of the ray from $P$, i.e., its angular departure from its ideal direction $PL$, is given by the slope of the wave front relative to the ideal sphere, namely $\partial OPD/\partial s$. The com-

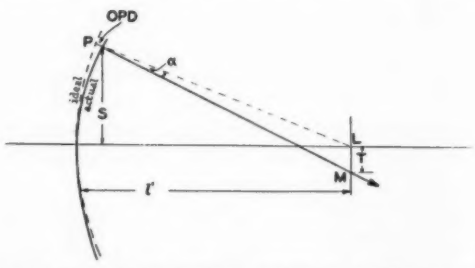


FIG. 1. The relation between optical path difference and transverse aberration.

[1] Gleichen, *Theory of Modern Optical Instruments*, p. 78.
[2] Conrady, *Applied Optics and Optical Design*, p. 277.
[3] Martin, *Applied Optics*, 1, 130. See also, Trans. Opt. Soc. 27, 96 (1925–6).
[4] Pelletan, *Optique Appliquée*, p. 58.

ponents of this angular aberration in the $x$ and $y$ directions are respectively

$$\alpha_x = \partial OPD/\partial x \qquad \text{and} \qquad \alpha_y = \partial OPD/\partial y.$$

The transverse displacement of the ray from its ideal position $L$ is $LM$, or $T$. This is negative when $\alpha$ is positive, as shown in Fig. 1, and thus $T = -l'\alpha = -l'(\partial OPD/\partial s)$. The $x$ and $y$ components of this are therefore,

$$x' = -l'(\partial OPD/\partial x), \text{ and } y' = -l'(\partial OPD/\partial y). \quad (2)$$

This gives the following values for the components of the ray displacement in the paraxial image-plane as

$$\left.\begin{aligned} x' &= -Ax(x^2+y^2) - 2Bxyh - Cxh^2 - Dxh^2, \\ y' &= -Ay(x^2+y^2) - B(x^2+3y^2)h \\ &\quad -3Cyh^2 - Dyh^2 - Eh^3. \end{aligned}\right\} \quad (3)$$

These equations may of course also be derived by a regular geometrical primary-approximation treatment of the action of a lens.[5]

The Eqs. (3) just derived are easier to discuss if we convert $x$ and $y$ into the corresponding polar coordinates $(s, \theta)$ of the point of emergence of the ray in the exit pupil (Fig. 2). To do this, write

$$x = s \sin\theta; \qquad y = s\cos\theta, \quad (4)$$

giving

$$\left.\begin{aligned} x' &= -As^3 \sin\theta - Bs^2h \sin 2\theta \\ &\quad - Csh^2 \sin\theta - Dsh^2 \sin\theta, \\ y' &= -As^3\cos\theta - Bs^2h(2+\cos 2\theta) \\ &\quad -3Csh^2\cos\theta - Dsh^2\cos\theta - Eh^3. \end{aligned}\right\} \quad (5)$$

## Image-Cone Sections in Paraxial Focal Plane for one Zone of a Lens

For a perfect lens, the image in the paraxial focal plane will be a point; in the presence of aberrations the image will be modified in the following way:

### A. Spherical aberration

For this aberration, taken alone, the coefficients $B$, $C$, $D$ and $E$ must be made equal to zero, and then the displacement components of the ray in the paraxial image plane become

[5] Conrady, M. N. Roy. Astron. Soc. 79, 64 (1918); and also see Czapski, *Grundzüge der Theorie der optischen Instrumente*, p. 151, 1904 edition; Southall, *Geometrical Optics*, p. 467; Glazebrook, *Dictionary of Applied Physics* 4, 313.

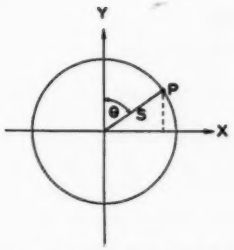


FIG. 2. Coordinates of a point in the exit pupil of the lens.

$$x' = -As^3 \sin\theta \qquad \text{and} \qquad y' = -As^3\cos\theta.$$

For any one zone, $s$ is constant, and consequently as $\theta$ varies from 0 to 360°, the point $(x', y')$ traces out a circle, centered about the Lagrangian image-point (Fig. 3). The diameter of this circle varies as $s^3$ for different zones.

### B. Coma

Here the coefficient is $B$, and the displacement components are

$$x' = -Bs^2h \sin 2\theta; \qquad y' = -Bs^2h(2+\cos 2\theta).$$

For any given zone $s$ and image-height $h$, these displacements plot as a double circle having a diameter of $2Bs^2h$, with its center at a distance $2Bs^2h$ below the Lagrangian image-point $L$. For a smaller zone, $s$ is less and the circle is therefore smaller and nearer to the point $L$, in such a way as always to fit against two common tangents at 60° to one another (Fig. 3).

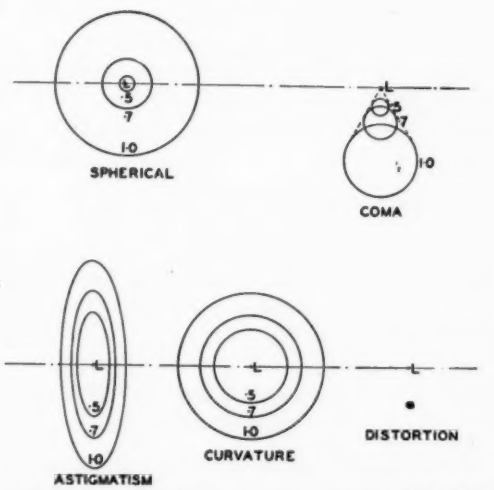


FIG. 3. Aberration cone sections in paraxial focal plane for three zones of the lens.

### C. Astigmatism

The displacements are now

$$x' = -Csh^2 \sin\theta \qquad \text{and} \qquad y' = -3Csh^2 \cos\theta.$$

This represents a vertical ellipse, centered about the Lagrangian image-point, and having a semi-major axis of $3Csh^2$ and a semi-minor axis of $Csh^2$ (Fig. 3). For other zones the ellipse is larger or smaller in proportion to $s$.

### D. Curvature of field

The displacements here are

$$x' = -Dsh^2 \sin\theta \qquad \text{and} \qquad y' = -Dsh^2 \cos\theta.$$

This represents a circle of diameter $2Dsh^2$ centered about the Lagrangian image point $L$. For other zones the circle changes in diameter in proportion to $s$.

### E. Distortion

Now

$$x' = 0 \qquad \text{and} \qquad y' = -Eh^3.$$

This represents a vertical displacement of the image point as a whole by an amount $Eh^3$, equally for all zones and all values of the parameter $\theta$.

## Cone Sections for Mixed Aberrations

These can be plotted trigonometrically in the same way as a single aberration, by using those terms having the coefficients of the aberrations it is desired to include. For example, a mixture of "equal" parts of coma and astigmatism is obtained by writing $A = D = E = 0$, and $B = C = 2$ (say). The ray displacement components are then found to be

$$x' = -2s^2h \sin 2\theta - 2sh^2 \sin\theta,$$

$$y' = -2s^2h(2 + \cos 2\theta) - 6sh^2 \cos\theta.$$

This plots as an oval with two little loops at the top (see the 5th section from the left in the middle row of Fig. 5).

## Graphical Construction for Cone Sections in Other Planes

If we know the values of $x'$ and $y'$ in one image plane, we can at once determine their values in any other plane shifted from the first by a distance ($kl'$), $k$ thus representing the ratio that the shift bears to the image-distance $l'$, by applying to the regular $x'$ and $y'$ the same terms as we found for a curvature of field, namely

$$x' = -k(s \sin\theta); \qquad y' = -k(s \cos\theta). \qquad (6)$$

For example, the shape of the cross section of the cone for pure coma, from a zone of unit radius at unit image height is

$$x' = -B \sin 2\theta - k \sin\theta,$$

$$y' = -B(2 + \cos 2\theta) - k \cos\theta.$$

This plots as a double looped figure (shown in Fig. 5, top row, fourth figure from the left).

The addition of the two $k$ terms can be done graphically by starting with an accurately computed figure, and by drawing straight lines from each point in the original figure, *sloping at an angle $\theta$ equal to the $\theta$ of that point* (see Fig. 4). A new series of points is then plotted by marking off distances $ks$ along these sloping lines, outwards for + values of $k$, and inwards for − values of $k$. A whole series of sections can therefore be plotted at once by marking off the corresponding values of $ks$ (plus or minus) along this one set of radial lines. Fig. 5 shows a complete array of cone sections for one zone for various proportions of coma and astigmatism at six positions along

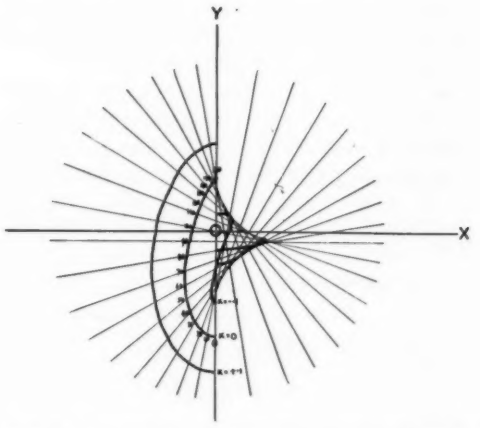


FIG. 4. Procedure for plotting cone sections at different distances along the axis given the computed section at one such distance. (This case represents a mixture of one "part" of coma and three "parts" of astigmatism.) Only one side of each figure need be plotted as they are all symmetrical about the vertical axis.

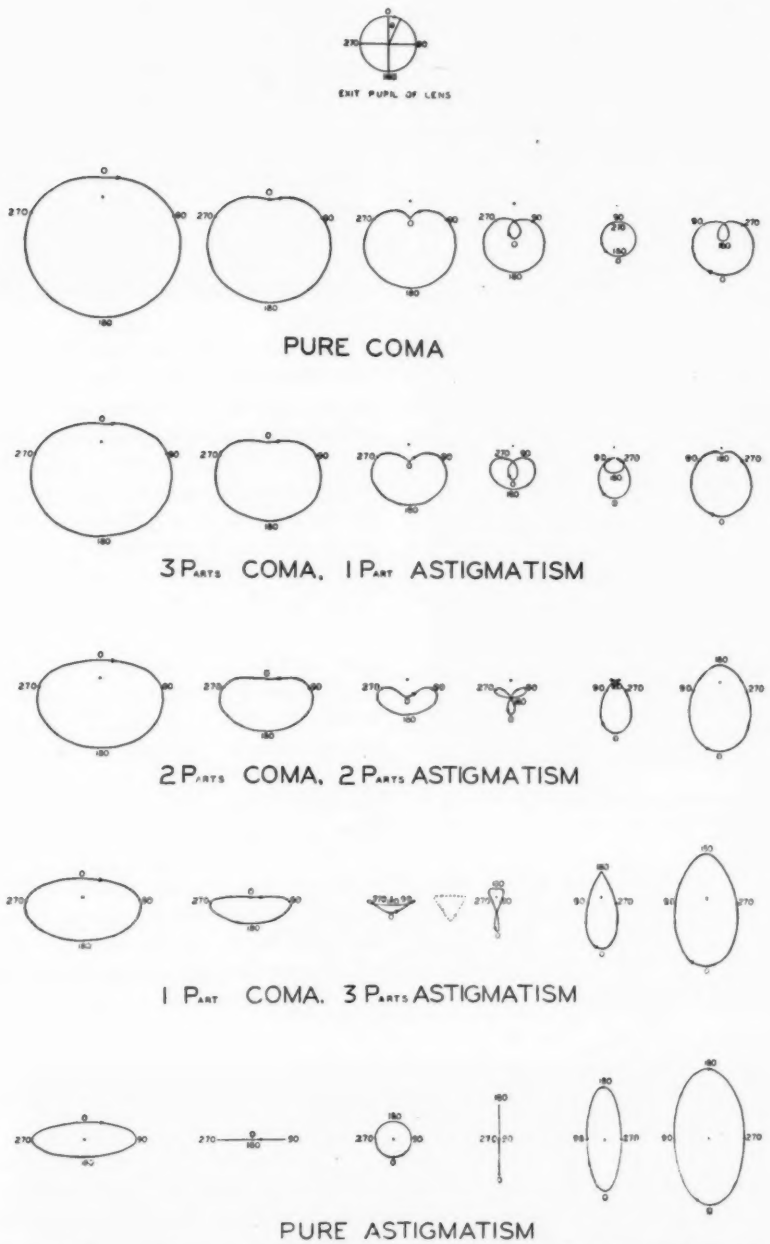
EXIT PUPIL OF LENS
PURE COMA
3 PARTS COMA, 1 PART ASTIGMATISM
2 PARTS COMA, 2 PARTS ASTIGMATISM
1 PART COMA, 3 PARTS ASTIGMATISM
PURE ASTIGMATISM

FIG. 5. Theoretical cross sections of image cone in the presence of coma and astigmatism.

the beam. Only the sections in the paraxial focal plane (for $k=0$) were computed, the others having been plotted graphically from them in this way.

Of course there are other ways[6] in which these figures may be derived but the one given is by far the neatest and simplest.

## Experimental Projection of these Cone Sections

If an achromatic doublet be rotated about a vertical axis through, say, 10 degrees, the resulting image of an object-point will of course have many aberrations of which by far the most prominent to an observer will be primary astigmatism and primary coma. By placing a negative cylindrical lens having no power along its vertical meridian in the path between object and achromat, primary astigmatism will be introduced in the beam of opposite sign to the astigmatism produced by the achromat. Obviously there will be a particular obliquity of the achromat such that the astigmatism thus produced will be exactly equal and of opposite sign to the astigmatism produced by the cylindrical lens. In this case the image will be free from primary astigmatism and the residual aberrations will, in general, as stated before, be very small and almost unnoticeable except for the primary coma. The ratio of astigmatism to coma in the final image may then be made anything from pure coma to pure astigmatism by varying the obliquity of the achromat from the above-mentioned case to zero obliquity where only the astigmatism produced by the cylinder will be evident.

In order to produce experimentally and verify the theoretical patterns (Fig. 5) of the sections of cones containing various ratios of coma to astigmatism from pure coma to pure astigmatism, the apparatus used consisted chiefly of a point source of light, a negative cylindrical lens, an achromatic lens with one or more zones isolated, a screen or photographic plate or paper and a suitable lens bench for holding the apparatus (Fig. 6). The point source consisted of a very

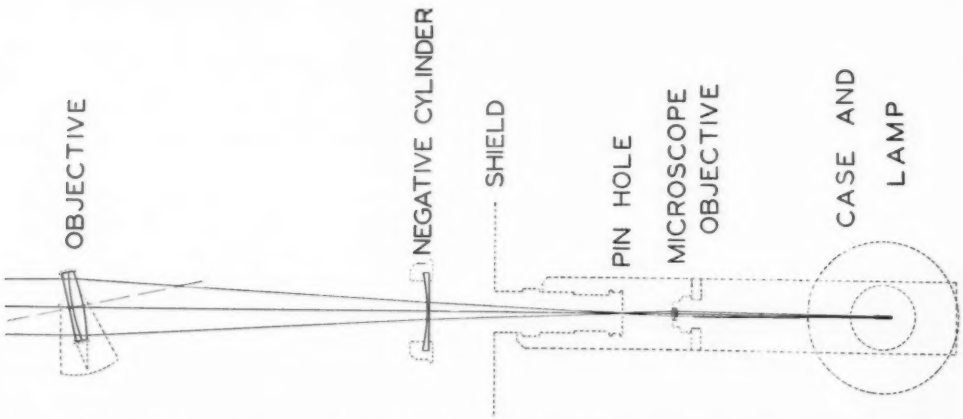


Fig. 6. Diagram of essential apparatus (with the exception of the projection screen which lies to the left of the diagram).

small pinhole in a piece of foil illuminated from behind by projecting on to it the image of a 250 watt projection lamp formed by a 32 mm microscope objective. To prevent stray light the lamp was encased in a coffee can, coated with dead black inside, with a round hole no larger than necessary to allow the light to enter the microscope objective. The mounting of the lamp, objective, pinhole and helpful shields to stop stray light is shown in the photograph of the apparatus (Fig. 7).

The negative cylindrical lens (a spectacle blank of 4 diopters power) was held in a mount

[6] Conrady, *Applied Optics and Optical Design*, p. 279.

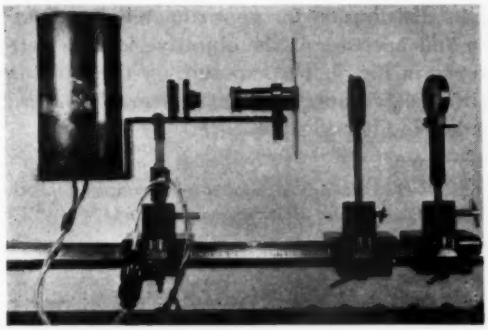

FIG. 7. Photograph of essential equipment used in producing various ratios of coma and astigmatism.

capable of being rotated about the optical axis of the lens. The achromat was mounted so that various obliquities could be given to it about a vertical axis of rotation. Several different achromats were used, varying in focal length of from 30 to 60 cm depending on the size of image desired, all of them 5.5 cm diameter. The single zones used had a width of about 1.5 mm.

It was found that for projection purposes where a large amount of aberration was desired, thus making the image appear larger, it was best to have that face of the achromat with the greater curvature toward the short conjugate. For full aperture the use of the achromat in this way would be unsatisfactory because of spherical aberration but for a marginal and a paraxial zone it was quite the better way of the two.

In cases where two or three or more marginal zones were used, because of the tedious process of cutting paper rings and attempting to glue them on the lens concentrically, the lens was slowly rotated in a lathe and the sections of the lens not wanted were painted with quick drying, rather thick, black Duco. Zones of remarkably good quality were obtained by this method after a few practice trials.

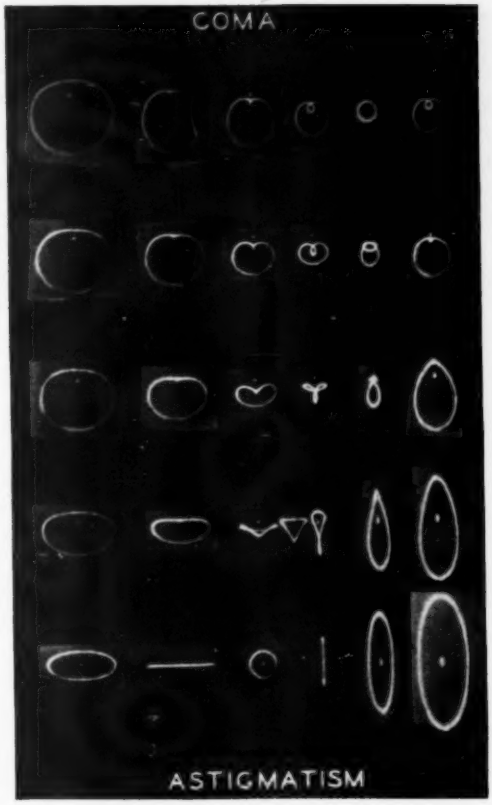


FIG. 8. Experimentally determined cone sections for one zone.

The actual photographs, taken individually

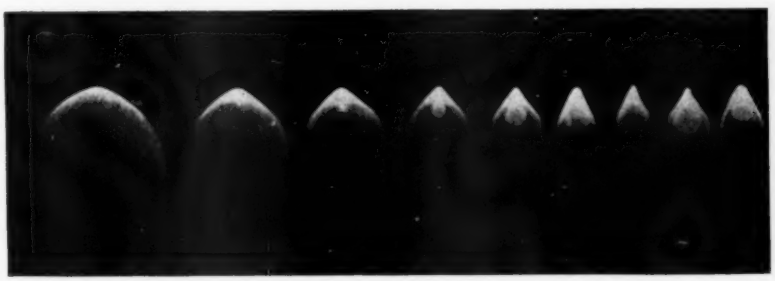

FIG. 9. Image cone sections for a complete lens, in presence of pure coma.

with an exposure of 25 seconds on Eastman P.M.C. No. 1 Bromide paper, are shown assembled in Fig. 8. A comparison of these photographs with the theoretically computed chart, Fig. 5, indicates that the experimental attempt at reproducing and verifying the theoretical patterns was quite successful, not only as to shape and size but also as to the light distribution. The light distribution for approximately pure coma for full aperture of the objective lens[7] is better shown in Fig. 9. The exposure for these pictures with the full aperture was decreased to 18 seconds. No filter was used.

[7] Gullstrand has given similar photographs for other aberrations, see Die Naturwissenschaften **14**, 664 (1926).

# A New Optical Experiment and the Use of a Single Lens for High Magnification; Observation of Entoptic and Diffraction Phenomena

J. GIBSON WINANS, *Department of Physics, University of Wisconsin*

(Received May 6, 1933)

An interesting optical experiment may be performed with a camera and converging lens. An extension of the experiment by use of the eye in place of the camera makes possible high magnifications with a single lens, location of flaws in glass, observation and location of particles within one's own eye and observation of Fresnel diffraction effects.

AN interesting optical experiment may be performed with a camera and converging lens. The arrangement is shown in Fig. 1. A spot of ink is drawn on the face of the camera lens $L$ and a star is drawn on the face of the converging lens $G$. The image of an incandescent lamp 15–20 feet away is focussed on the camera ground glass with $L$ alone and the starred lens $G$ is held between lens $L$ and the source. Distinct images of both spot and star appear on the ground glass. Now lens $G$ is moved in *any* direction but the star image remains fixed in position and constant in size independent of the motion of the star itself. The only motion of the star which is followed by the star image is one of rotation. The image of the spot, however, follows the motion of $G$ though the spot itself is stationary. Motion of $G$ along $GK$ causes a displacement of the spot image and motion along $GS$ causes the spot image first to grow very large and then to diminish, approaching zero size as a limit.

This experiment may be performed with the eye replacing the camera if a point source is used.

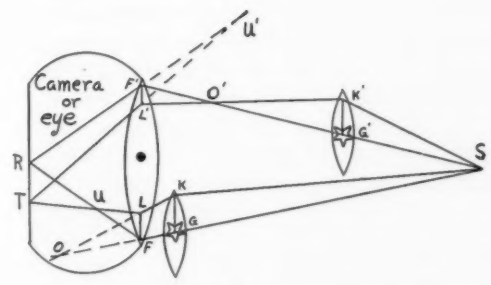


FIG. 1.

The observer sees the star image which does not move with motion of $G$ and sees also shadow images of various objects within his own eye. He may observe the contraction of his own iris by turning on a light near the eye.

These experiments are more striking when observed than when described. For maximum enjoyment the reader should try them.

The explanation follows readily from Fig. 1. Two positions, $G$ and $G'$, are shown for the lens. Light from $S$ after passing lenses $G$ and $L$ converges through point $U$ to give a large blur circle on the retina or ground glass $RT$. Point $U$ acts like a pinhole aperture and produces a shadow image on $RT$ of any object between $R$ and $S$, including the spot on $L$ and the star on $G$. Let $F$ represent the point where a ray of light through the center of $G$ strikes lens $L$. Since light from $S$ would be focussed by lens $L$ at $R$, a ray of light through the center of $G$, not being deviated by $G$, is directed by Lens $L$ to point $R$ regardless of the position of $G$ itself. Therefore the center of the star image remains fixed and independent of any motion of lens $G$. Let $GK$ be the length of the star object so that $RT$ is the length of the star image. Then from Fig. 1

$$RT/LF=RU/UF \quad (1) \qquad LF/GK=OF/OG \quad (2)$$

and from the lens equation

$$\mp(1/OF)\pm(1/UF)=(1/f), \qquad (3)$$

where $f$ is the focal length of lens $L$. The upper sign is for position $G$ and the lower for $G'$. Combining (1), (2), and (3) gives the magnification as

$$m\equiv RT/GK=(RU/OG)(f/f\mp UF). \qquad (4)$$

If the source is a long way off, $OG$ equals the focal length of $G=g$, and $RU=f\mp UF$. Substituting in (4) gives $m=f/g$. The magnification depends only on the focal lengths of the two lenses and is independent of the position of $G$. Therefore the size as well as the position of the star image is independent of any motion of lens $G$. The position and size of the spot image depends on the position of point $U$ and is determined by the pinhole camera relation.

If an object is placed at point $I$, Fig. 2, it can be shown by an argument similar to that above

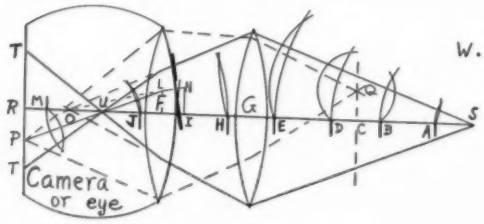


FIG. 2.

that the position and size of its image is independent of any motion of the object and lens $G$, provided that the length $IG$ is constant in magnitude and direction. The size of the image is determined by $f$, $g$, and the distance $IG$.

## HIGH MAGNIFICATION WITH A SINGLE LENS

Since any object between $R$ and $S$, Fig. 2, gives a shadow image on the retina, a slide held at any place between the eye and the source will be seen distinctly. With a distant point source and the slide in contact with $G$, the magnification is exactly the same as though $G$ were used as a simple magnifier (i.e., with the slide at $C$, Fig. 2). Placing the slide in contact with $G$ has the advantage that any motion of the lens and slide produces no motion of the image on the retina. When the slide is moved from $G$ to $E$, $D$, $C$, $B$, and $A$, Fig. 2, the image remains constant in size. When the slide is moved from $G$ to $H$ and $I$, and lens $G$ moved toward $S$ so that point $U$ approaches the slide, the image starts at the simple magnifier size and grows very large. A total magnification of over 80 diameters was obtained with a single camera lens of focal length 10 cm.

By using this principle, an ordinary camera may be converted into a low power microscope. A hole about the diameter of the lens is bored or punched in the back of a plateholder and metal strips fastened to the holder to support a slide over the hole. With the plateholder and slide in place, the camera is supported between the eye and a point source of light. The observer sees an enlarged image of the slide. The magnification is controlled by varying the distance between the camera lens and slide. The resolving power is low but increases with magnification as will be shown later. This camera microscope may be found useful for observations where magnification rather than resolving power is needed.

## TEST FOR FLAWS IN GLASS

Since any object or speck between $R$ and $S$ of Fig. 1 casts a shadow image on the retina, a flaw in lens $G$ or in a plate of glass in contact with $G$ will be observed along with irregularities in the eye. Images of flaws in the lens or glass remain stationary when the lens and glass are moved in any direction. A test similar to this was described by Glazebrook.[1]

Flaws in the polish of converging spectacle lenses may be observed by holding the lens between the eye and a distant light. Light which reflects twice within the lens enters the eye as though from a strong lens and produces a blur circle on which may be seen the imperfections of polish.

## ENTOPTIC PHENOMENA

It is well known that shadows of particles on and within one's own eye may be observed by holding a point source of light close to the eye, or by looking through a high power microscope. This is known as entoptic phenomena.[2] The arrangement of Fig. 1 is very good for entoptic observations since any object in the eye will cast a shadow image on the retina. The relative position of objects may be ascertained by moving lens $G$ along $GK$. Images which move with $G$ are of objects between $U$ and $L$ while images which move opposite to $G$ are of objects between $U$ and $R$, but since images on the retina always appear to move opposite to their actual motion, the images of objects between $R$ and $U$ appear to move with $G$.

[1] Glazebrook, *Dictionary of Applied Physics* **4**, 402.

[2] H. v. Helmholtz, *Physiological Optics* **1**, 204.

Images of water drops on the eye appear as black circles when point $U$, Fig. 1, is inside the eye and as bright spots when $U$ is outside the eye. This is due to the lens action of the drops which throws light into or outside of the geometrical shadow when $U$ is outside or inside the eye respectively.

Professor J. E. Mack has pointed out to the writer that the virtual image of a distant light in a steel ball is a good source for observing entoptic phenomena. If the distant light is an open carbon arc, the observer sees also a greatly magnified and brilliantly colored image of the *surface of the ball*. The magnification is due to the nearness of the surface to the virtual source. The only motion of the ball followed by the image is one of rotation.

Entoptic phenomena may be demonstrated to an entire class by having each student look at a brightly illuminated screen through a pinhole in a card.

## Diffraction Effects

The arrangement of Fig. 2 was used by Michelson[3] for observing diffraction patterns surrounding particles within the eye. It may also be used to observe diffraction from obstacles outside of the eye. Diffraction patterns are observed surrounding the images of objects placed at any point between the eye and the source except point $C$. Point $C$ is the simple magnifier position. When an object is moved from $E$ to $D$, $C$, $B$, and $A$, the fringes narrow, disappear for position $C$, then reappear and widen for positions $B$ and $A$. When the object moves from $H$ to $I$, $J$, $U$, $M$ to $R$, the fringes widen, approaching infinite separation for position $U$, then shrink to infinitesimal separation for position $R$. Various obstacles such as wedges, slits, circles, and edges may be drawn on paper and photographed. The diffraction from all obstacles may be observed simultaneously by holding the negative in contact with lens $G$. This is a convenient method of observation since movement of the lens and plate produces no motion of the images or their fringes.

The diffraction fringes are of the Fresnel type and may be explained as follows. Consider the illumination at point $P$, Fig. 2. If $P$ were a light source, waves would diverge from $P$, pass through $F$, converge toward $W$, pass through $G$ and converge through $Q$ as shown by dotted lines. Spherical shells with $P$, $W$ or $Q$ as centers show the positions of equal optical distance from $P$. The actual light waves diverge from $S$, pass $G$, converge toward $O$, pass $F$, and converge through $U$ as shown in Fig. 2. Spherical shells with $S$, $O$ or $U$ as centers show points of equal phase. Consider a straight edge obstacle at some point, e.g., $B$, Fig. 2. The shells of equal phase and equal distance are drawn with the circle of intersection tangent to the obstacle. The illumination at $P$ will be a maximum or minimum when the number of Fresnel zones included in the circle of intersection is odd or even, respectively. The wave outside of the circle adds slightly to the intensity at $P$ without changing its character as a maximum or minimum.[4] The number of zones in the circle of intersection is $n=2s/\lambda$ where $s$ is the maximum distance between the shells and $\lambda$ is the wave-length of light in the medium at $B$. $n$ also equals the number of maxima and minima between $P$ and $R$.

To find $s$, construct a triangle between the edge $b$ at the point of tangency and the centers of the two arcs $Q$ and $S$. $s=SB+BQ-QS$. In general, for any position of the obstacle such as $A$, $D$, $E$, $H$, $I$, $J$, or $M$, Fig. 2, construct a triangle between the obstacle and the centers of the shells of equal phase and equal distance. Let $\gamma$ be the long side of this triangle and $\alpha$ and $\beta$ be the two short sides. Then $s=\alpha+\beta-\gamma$ and $n=(2/\lambda)(\alpha+\beta-\gamma)$. $n$ is the number of maxima and minima between $P$ and $R$. $\alpha$, $\beta$, and $\gamma$ are obtained by measurement.

The fringes disappear for an edge at $C$ because $n=(2/\lambda)(QC+CS-QS)$, a very large number. The fringes become very wide for an obstacle at $U$ since $n=(2/\lambda)(PU+O-PU)=0$.

When $n$ is known, the complete pattern showing positions and relative intensities of all the maxima may be calculated from Cornu's spiral by using $n$ and $RP$ to convert the scale of the spiral to that of the apparatus. Diffraction from other types of obstacles may be figured from Cornu's spiral.[5] Michelson[3] calculated the pattern surrounding small circular particles in the eye between $U$ and $R$.

[3] A. A. Michelson, J. O. S. A. 9, 197 (1924).

[4] R. W. Wood, *Physical Optics*, p. 244.

[5] Reference 4, p. 192.

### Resolving Power of Camera Microscope

For a microscope to resolve two slits, the separation between the slit images must equal or exceed the separation of the central maximum and first minimum for one of the slits. Consider a slit at $I$, Fig. 2, of width $t$. If $t$ is less than the diameter of the first zone, $P$, the center of the slit image will be a point of maximum intensity. For the first minimum to fall at $R$, one edge of the slit must be $\lambda$ farther from $R$ than the other. The shell of equal distance from $R$ is shown in Fig. 2. From Fig. 2,

$$\lambda/t = NI/OI = LF/OF \quad (5) \qquad RU/UF = RP/LF \quad (6)$$

$$-1/OF + 1/UF = 1/f. \quad (7)$$

Combining gives

$$RP = f\lambda/t. \quad (8)$$

If there are two slits of width $t$, separated $r$ cm, they will be just resolved when $RP$ is the distance between their images. Let $r = NI$ in Fig. 2. From (5), (6), and (7) by using $RU = f - UF$ as for a distant source,

$$m = RP/r = f/Oi. \quad (9)$$

Combining with (8) gives

$$r = OI\lambda/t \quad (7) \qquad \text{or} \qquad m = f\lambda/rt. \quad (8)$$

$m$ is the magnification necessary to resolve the slits. It depends directly on $f$, the focal length of the eye lens. If $f$ is decreased by inserting a strong converging lens between $F$ and $I$ the magnification needed for resolution should be decreased and the resolving power correspondingly increased. Experiment showed this to be true. Measurements made to check Eq. (7) are given in Table I.

Table I. *Slit width, 0.042 mm. Wave-length, 5460A.*

| $OI$ (mm) | Limit of resolution, $r$ Calculated (mm) | Observed (mm) |
|---|---|---|
| 31.1 | 0.41 | 0.45 |
| 29.7 | 0.35 | 0.43 |
| 25.5 | 0.33 | 0.36 |
| 19.1 | 0.25 | 0.30 |
| 15.2 | 0.22 | 0.24 |
| 14.9 | 0.19 | 0.22 |

The calculated and observed values of $r$ agree sufficiently well to show that the theory is correct. The observed limits of resolution were larger than the calculated by about the slit width. This is probably due to the tendency in measurement to consider the slits unresolved as soon as their images overlap.

The experiments described above may be used as a laboratory experiment, as an aid in locating flaws in lenses and flaws in the eye, as a convenient method for studying Fresnel diffraction effects and as a substitute for a microscope when high resolving power is not required.

# Optical Tests of the 69-Inch Perkins Observatory Reflector

HARLAN T. STETSON, *Perkins Observatory, Delaware, Ohio*

(Received May 24, 1933)

The large disk of glass cast by the Bureau of Standards in May, 1927, has emerged into the completed paraboloidal reflector which has been placed in the Perkins Observatory telescope at Delaware, Ohio. Before removal of the glass to Delaware, an extensive series of optical tests were made in the testing laboratory of the J. W. Fecker Company, in Pittsburgh, where the optical surface of the mirror was ground and figured. The final tests were carried on over a period of five days, Dr. J. S. Plaskett, director of the Dominion Astrophysical Observatory, and Dr. I. G. Gardner, of the Bureau of Standards, cooperating. Some 3000 settings were made by the knife-edge test at the center of curvature. Excellent agreement was found among the different observers. Computed results show the mean focal length of the mirror to be 24 feet $11\frac{3}{4}$ inches and the departures from this value for different zones of varying radii to be not over one-tenth of a millimeter as would be tested in parallel light reflected to a focus. Tests were also made by the Hartmann method and a comparison made between the results of the two methods. The value of the Hartmann criterion for the mirror from laboratory tests is placed at 0.14.

WITH the completion of the figuring of the 69-inch mirror in 1931 at the factory of the J. W. Fecker Company, Pittsburgh, the mirror was carefully subjected to laboratory tests both by the knife-edge and the Hartmann methods before its removal to Delaware, Ohio.

By invitation, Dr. I. G. Gardner, chief of the division of optical instruments of the Bureau of Standards, and Dr. J. S. Plaskett, director of the Dominion Astrophysical Observatory, participated with the director of the Perkins Observatory in a five-day session of optical tests in Pittsburgh to determine the excellence of the finished surface, from November 12 to 16. The tests were carried on in the testing tunnel which was constructed with reasonable insulation to insure constant temperature. A thermograph set up close by the mirror revealed temperature changes of less than 1°C during the five days of the test, the mean temperature being approximately 18.3°C (65°F).

In the knife-edge tests the knife-edge was placed at the center of curvature alongside the artificial star illuminated by an Argand burner. A support for the knife-edge was built especially for the purpose, entirely of metal and capable of movement through milled slides along the optical axis of the mirror and horizontally at right angles to this line. The mirror itself during the tests was covered with a wall board diaphragm containing twenty apertures, rectangular in shape, with appropriate flaps opened and closed by cords extending to the observing end of the tunnel. The apertures were opened by pairs exposing successive zones in order from the one nearest the periphery to the one nearest the central hole which had been cut for the Cassegrain combination, the hole in the mirror being approximately 9 inches in diameter. The radii of the several zones, measured from the optical center of the mirror to the middle of the appropriate rectangular aperture, are given in Table I together with the theoretical focal differences based on the computation of the aberration of a paraboloid at the center of curvature, only the first aberrational term $r^2/R$ being used, where small $r$ is the radius of the zone and large $R$ the radius of curvature of the mirror. Higher order terms of the formula

TABLE I. *Knife-edge test.*

| Zones | Radii (inches) | Radii (mm) | $r^2$ (mm) | $r^2/R$ | Theoretical differences |
|---|---|---|---|---|---|
| 1 | 33.75 | 857.2534 | 734883.39 | 48.260 | 0.000 |
| 2 | 30.75 | 781.0530 | 610043.79 | 40.062 | 8.198 |
| 3 | 27.75 | 704.8528 | 496817.47 | 32.626 | 15.634 |
| 4 | 24.75 | 628.6524 | 395203.84 | 25.953 | 22.307 |
| 5 | 21.75 | 552.4522 | 305203.43 | 20.042 | 28.218 |
| 6 | 18.75 | 476.2518 | 226815.78 | 14.895 | 33.366 |
| 7 | 15.75 | 400.0516 | 160041.28 | 10.510 | 37.750 |
| 8 | 12.75 | 323.8512 | 104879.60 | 6.887 | 41.373 |
| 9 | 9.75 | 247.6510 | 61331.02 | 4.027 | 44.233 |
| 10 | 6.75 | 171.4506 | 29395.31 | 1.930 | 46.330 |
| | | 5143.5200 | | | |

$F$ = 24 ft. 11.75 inches $R = 2F = 15227.36$ mm

$\rho = R + r^2/R + r^4/8R^3$ were omitted as computation showed them to be negligible.

In making the settings the knife-edge was adjusted so that a uniform darkening occurred in the beams from both of the members of the pair of rectangular apertures involved. Then a scratch was made by means of a steel scriber bearing against a movable index attached to the knife-edge support and leaving its trace upon a removable brass strip clamped between fixed stops on a stationary metal plate. Two settings were made on each zone at a time, the mean position of the two scratches later measured being taken for the focal center of that zone. In this way a complete run could be made on all zones of the mirror at one sitting without interruption or distracting illumination for the reading of scales or micrometer screw. This method also served to remove completely any prejudice on the part of the observer from previously made readings. The locations of the several settings were then determined conveniently in daylight by suitable juxtaposition of the inscribed brass strips against a standard steel scale.

Table II gives the results of a series of six settings by zones on November 12 by two of the observers. The readings are entered in an arbitrary scale with tenths of millimeters as units, the means for each of the ten zones being then expressed in millimeters. To adjust the arbitrary scale to zero for the first zone the mean reading for the first zone, 15.366 (Stetson) or 15.850 (Plaskett), is subtracted from the mean settings of the zones in order. Comparison of these reduced means with the computed aberration $r^2/R$ at once follows in the row of differences. To distribute plus and minus signs equally in these differences the mean residual, $-1.044$ (Stetson) or $-0.932$ (Plaskett), is applied to each of the ten zones.

It is to be noted that since the observations were made at the center of curvature the equivalent differences for parallel light received at the focus will be equal to the differences tabulated at the center of curvature, $C_0$, divided by the factor four. The last line of the table for each observer therefore represents the residuals measured at the center of curvature divided by four to reduce to the residuals $(F - F_0)$ that would be obtained from parallel light at the focus.

The probable error for each observer, computed from a series of sixty continuous settings, was determined with the following values for the probable error for a single setting at the center of curvature: Hageman, 0.272; Plaskett, 0.186; Stetson, 0.232.

In Table III is printed a summary of all observations made by the several observers. Column

TABLE II. *Knife-edge tests of 69-inch mirror made in Pittsburgh on November 12, 1931.*

| Horizontal axis (mirror 0°–180°) Zones | 1 | 2 | 3 | 4 | 5 | 6 | 7 | 8 | 9 | 10 |
|---|---|---|---|---|---|---|---|---|---|---|
| *Stetson* | | | | | | | | | | |
| | 155 | 230 | 304 | 371 | 428 | 471 | 519 | 554 | 578 | 606 |
| | 155 | 234 | 304 | 371 | 430 | 472 | 521 | 556 | 586 | 613 |
| | 144 | 230 | 300 | 360 | 421 | 470 | 512 | 548 | 578 | 603 |
| | 156 | 231 | 301 | 368 | 426 | 470 | 513 | 552 | 583 | 608 |
| | 159 | 231 | 303 | 364 | 426 | 468 | 513 | 551 | 588 | 597 |
| | 153 | 235 | 301 | 365 | 423 | 470 | 515 | 556 | 588 | 600 |
| mean (mm) | 15.366 | 23.183 | 30.216 | 36.650 | 42.566 | 47.016 | 51.550 | 55.283 | 58.350 | 60.450 |
| −15.366 | 0.000 | 7.817 | 14.850 | 21.284 | 27.200 | 31.650 | 36.184 | 39.917 | 42.984 | 45.084 |
| $r^2/R$ | 0.000 | 8.198 | 15.634 | 22.307 | 28.218 | 33.366 | 37.750 | 41.373 | 44.233 | 46.330 |
| Diff. | 0.000 | −0.381 | −0.784 | −1.023 | −1.018 | −1.716 | −1.566 | −1.456 | −1.249 | −1.246 |
| mean | −1.044 | | | | | | | | | |
| Resid. at $C_0$ | 1.044 | 0.663 | 0.260 | 0.021 | 0.026 | −0.672 | −0.522 | −0.412 | −0.205 | −0.202 |
| ÷4; $(F-F_0)$ | 0.261 | 0.166 | 0.065 | 0.005 | 0.007 | −0.168 | −0.131 | −0.103 | −0.051 | −0.051 |
| *Plaskett* | | | | | | | | | | |
| | 153 | 236 | 311 | 372 | 432 | 482 | 523 | 561 | 591 | 611 |
| | 160 | 237 | 307 | 374 | 431 | 481 | 522 | 551 | 589 | 617 |
| | 159 | 233 | 308 | 369 | 433 | 472 | 519 | 550 | 590 | 618 |
| | 160 | 232 | 309 | 372 | 433 | 479 | 521 | 560 | 596 | 610 |
| | 160 | 233 | 307 | 372 | 430 | 477 | 526 | 556 | 589 | 607 |
| | 159 | 233 | 307 | 372 | 435 | 479 | 521 | 559 | 593 | 616 |
| mean (mm) | 15.850 | 23.400 | 30.816 | 37.183 | 43.233 | 47.833 | 52.200 | 55.616 | 59.133 | 61.316 |
| −15.850 | 0.000 | 7.550 | 14.966 | 21.333 | 27.383 | 31.983 | 36.350 | 39.766 | 43.283 | 45.466 |
| $r^2/R$ | 0.000 | 8.198 | 15.634 | 22.307 | 28.218 | 33.366 | 37.750 | 41.373 | 44.233 | 46.330 |
| Diff. | 0.000 | −0.648 | −0.668 | −0.974 | −0.835 | −1.383 | −1.400 | −1.607 | −0.950 | −0.864 |
| mean | −0.932 | | | | | | | | | |
| Resid. at $C_0$ | 0.932 | 0.284 | 0.264 | −0.042 | 0.097 | −0.451 | −0.468 | −0.675 | −0.018 | 0.068 |
| ÷4; $(F-F_0)$ | 0.233 | 0.071 | 0.066 | −0.011 | 0.024 | −0.113 | −0.117 | −0.169 | −0.005 | 0.017 |

TABLE III. *Results of knife-edge test of the 69-inch mirror based on measurements made November 12 to 16, 1931.*

| Zones | | Plaskett | Stetson | $(F-F_0)$ | $r^2(F-F_0)$ | $(F-F_0)-0.06$ | $r^2[(F-F_0)-0.06]$ |
|---|---|---|---|---|---|---|---|
| *Axis AB Horizontal* | | | | | | | |
| 1 | | 0.233 | 0.261 | 0.245 | 180046 | 0.185 | 135953 |
| 2 | | 0.071 | 0.166 | 0.113 | 68935 | 0.053 | 32332 |
| 3 | | 0.066 | 0.065 | 0.066 | 32790 | 0.006 | 2981 |
| 4 | | −0.011 | 0.005 | −0.004 | 1581 | 0.064 | 25293 |
| 5 | | 0.024 | 0.007 | 0.016 | 4883 | 0.044 | 13429 |
| 6 | | −0.113 | −0.168 | −0.137 | 31074 | 0.197 | 44683 |
| 7 | | −0.117 | −0.131 | −0.123 | 19685 | 0.183 | 29288 |
| 8 | | −0.169 | −0.103 | −0.140 | 14683 | 0.200 | 20976 |
| 9 | | −0.005 | −0.051 | −0.025 | 1533 | 0.085 | 5213 |
| 10 | | 0.017 | −0.051 | −0.013 | 382 | 0.073 | 2146 |
| | | | | $\Sigma r^2(F-F_0)$ | 355592 | | 312294 |
| | | | | | $T=0.2385$ | | 0.2095 |
| *Axis CD Horizontal* | | | | | | | |
| 1 | 0.123 | 0.159 | 0.187 | 0.158 | 116112 | 0.098 | 72019 |
| 2 | 0.029 | 0.093 | 0.137 | 0.089 | 54294 | 0.029 | 1769 |
| 3 | 0.039 | 0.059 | 0.047 | 0.050 | 24841 | 0.010 | 4968 |
| 4 | 0.096 | 0.032 | 0.038 | 0.052 | 20551 | 0.008 | 3162 |
| 5 | 0.043 | −0.021 | −0.005 | 0.002 | 610 | 0.058 | 17702 |
| 6 | −0.088 | −0.175 | −0.074 | −0.118 | 26764 | 0.178 | 40373 |
| 7 | −0.153 | −0.279 | −0.232 | −0.229 | 36649 | 0.289 | 46252 |
| 8 | −0.158 | −0.126 | −0.225 | −0.167 | 17515 | 0.227 | 23808 |
| 9 | 0.014 | 0.242 | 0.072 | 0.124 | 7605 | 0.064 | 3925 |
| 10 | 0.053 | 0.018 | 0.054 | 0.039 | 1146 | 0.021 | 617 |
| | | | | $\Sigma r^2(F-F_0)$ | 306087 | | 230517 |
| | | | | | $T=0.2053$ | | 0.1546 |
| Combining the residuals $(F-F_0)$ for the two axes, the mean value of $T=0.2200$ | | | | | | | 0.1778 |

five gives the mean value of $(F-F_0)$ based on the results of the several observers weighted inversely as their probable errors. From these results the Hartmann criterion was calculated as follows:

$$T=200{,}000\,\Sigma r^2(F-F_0)/(F_m{}^2\Sigma r).$$

If the residuals are weighted by the light-gathering power of the zone, that is by multiplying by $r^2$, it was found that by shifting the focal plane $F_0$ by 0.06 mm $\Sigma rd/\Sigma r$ could be reduced to a minimum in accordance with Hartmann's procedure for weighting the residuals by the light-gathering power of the zone. The resulting values of $T$ are shown respectively for the two axes of the mirror $AB$ and $CD$. As it was impractical to take zonal readings in a vertical direction the mirror was turned through 90° and allowed to rest over night between the series of measures.

For purposes of obtaining Hartmann plates for zonal errors the wall board screen in front of the mirror was replaced by a diaphragm of heavy paper containing forty holes representing two pairs of rectangular axes with ten holes in each axis. The radii of the zones are given in Table IV.

TABLE IV. *Hartmann test.*

Axis $AB$ (horizontal)
Axis $CD$ (vertical)

| Zones | Radii in mm | | $r^2$ mm | | $r^2/R$ | |
|---|---|---|---|---|---|---|
| | $AB$ | $CD$ | $AB$ | $CD$ | $AB$ | $CD$ |
| 1 | 857.55 | 858.55 | 735392.00 | 737108.10 | 48.294 | 48.407 |
| 2 | 781.35 | 781.55 | 610507.82 | 610820.40 | 40.093 | 40.113 |
| 3 | 704.95 | 705.95 | 496594.50 | 498365.40 | 32.636 | 32.728 |
| 4 | 628.95 | 629.15 | 395578.10 | 395829.72 | 25.978 | 25.995 |
| 5 | 552.55 | 553.55 | 305311.50 | 306417.60 | 20.050 | 20.123 |
| 6 | 476.55 | 476.35 | 227099.90 | 226909.32 | 14.914 | 14.901 |
| 7 | 400.05 | 400.55 | 160040.00 | 160440.30 | 10.510 | 10.536 |
| 8 | 323.85 | 323.95 | 104878.82 | 104943.60 | 6.888 | 6.892 |
| 9 | 247.75 | 247.75 | 61380.06 | 61380.06 | 4.031 | 4.031 |
| 10 | 171.45 | 171.55 | 29395.10 | 29429.40 | 1.930 | 1.933 |
| $\Sigma r$ = | 5145.00 | 5148.90 | | | | |

$F=24$ ft. 11.75 inches $R=2F=15227.36$ mm

Four plates were exposed, two inside and two outside the focus. The plates were taken and measured by Dr. Plaskett. Detailed accounts of the Hartmann method have already been published and a summary of the results for the 69-inch mirror therefore appears sufficient in giving the results of the present test. (See Table V.)

As in the case of the knife-edge, the measures at the center of curvature were reduced to parallel light at the focus, the focal plane $F_0$ being so adjusted as again to render $\Sigma rd$ a minimum.

TABLE V. *Results of Hartmann test of the 69-inch mirror.**

| Zones | $(F-F_0)$ | $r^2(F-F_0)$ | $(F-F_0)-0.06$ | $r^2[(F-F_0)-0.06]$ |
|---|---|---|---|---|
| *Axis AB Horizontal* | | | | |
| 1 | 0.074 | 54482 | 0.014 | 10308 |
| 2 | −0.129 | 78776 | 0.189 | 115416 |
| 3 | 0.039 | 19398 | 0.021 | 10445 |
| 4 | −0.072 | 28491 | 0.132 | 52233 |
| 5 | 0.091 | 27834 | 0.031 | 9482 |
| 6 | −0.137 | 31100 | 0.197 | 44720 |
| 7 | −0.056 | 8973 | 0.116 | 18588 |
| 8 | −0.051 | 5350 | 0.111 | 11645 |
| 9 | 0.097 | 5954 | 0.037 | 2271 |
| 10 | 0.143 | 4206 | 0.083 | 2441 |
| | $\Sigma r^2(F-F_0)$ | 264564 | | 277549 |
| | | $T=0.1774$ | | 0.1861 |
| *Axis CD Vertical* | | | | |
| 1 | 0.059 | 43439 | 0.001 | 736 |
| 2 | 0.264 | 161215 | 0.204 | 124575 |
| 3 | 0.148 | 73612 | 0.088 | 43769 |
| 4 | 0.148 | 58564 | 0.088 | 34822 |
| 5 | 0.036 | 11011 | 0.024 | 7341 |
| 6 | −0.223 | 50622 | 0.283 | 64242 |
| 7 | −0.308 | 49354 | 0.368 | 58968 |
| 8 | −0.255 | 26752 | 0.315 | 33047 |
| 9 | 0.045 | 2762 | 0.015 | 921 |
| 10 | 0.086 | 2529 | 0.026 | 765 |
| | $\Sigma r^2(F-F_0)$ | 479860 | | 369186 |
| | | $T=0.3217$ | | 0.2475 |
| Combining the residuals $(F-F_0)$ for both axes, | | $T=0.1780$ | | 0.1034 |

* Plates were taken and measured in Pittsburgh in November 1931, by Dr. Plaskett.

FIG. 1.

In calculating $T$ from the Hartmann plates, the horizontal and vertical axes were combined and gave a value of $T=0.103$ as compared with the value of $T$ determined from the two axes measured in the horizontal direction in the knife-edge method of 0.178. Giving equal weight to the Hartmann and knife-edge methods the final accepted value of the mean weighted diameter of the confusion disk in units of one-one hundred thousandths of the focal length as defined by Hartmann is $T=0.14$ which places the excellence of the optical work according to Hartmann's classification of the highest order.

In addition to the knife-edge and Hartmann plates, a careful inspection of the mirror with the knife-edge test at the principal focus was made by Gardner, Plaskett and Stetson, utilizing the large flat which covered about half of the aperture of the 69-inch mirror at the time. No appreciable irregularities were detected by this method.

The apparent small amount of astigmatism found in comparing the focus in the vertical and horizontal axes of the Hartmann test plates was believed to be due to air turbulence in the tunnel in the vertical direction. When the mirror was turned through 90°, knife-edge tests showed no such asymmetry in the axes. All knife-edge readings were made along a horizontal diameter at right angles to the optical axis of the mirror.

Stellar photographs obtained at the observatory since the mirror has been at work in the telescope, as exhibited in the accompanying photograph of Messier 8 (Fig. 1), remove all doubt that the astigmatism indicated between vertical and horizontal axes measured in the

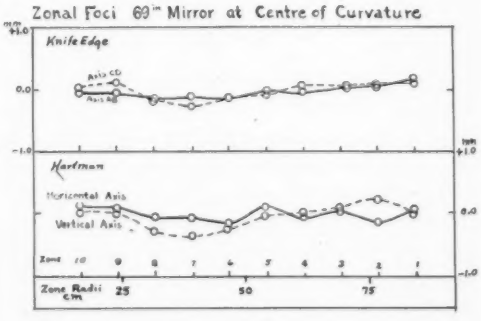


FIG. 2.

tunnel was due to the vertical temperature gradient. Temperature readings in the tunnel showed a difference of 2°F between the bottom and the top of the mirror during the tests. The reasonable agreement of the Hartmann criterion $T$ for parallel light reduced to a focus both in the case of the Hartmann plates and the knife-edge test, indicates the optical excellence of the finished product. The graph showing the zonal differences actually measured is shown in Fig. 2.